The Astrophysical Journal, 686:1231–1244, 2008 October 20

PERPENDICULAR TRANSPORT OF ENERGETIC CHARGED PARTICLES IN NONAXISYMMETRIC TWO-COMPONENT MAGNETIC TURBULENCE

D. Ruffolo,[1] P. Chuychai,[2] P. Wongpan,[1] J. Minnie,[2] J. W. Bieber,[2] and W. H. Matthaeus[2]
Received 2008 April 26; accepted 2008 July 1

ABSTRACT

We examine energetic charged particle diffusion perpendicular to a mean magnetic field $\boldsymbol{B}_0$ due to turbulent fluctuations in a plasma, relaxing the common assumption of axisymmetry around $\boldsymbol{B}_0$ and varying the ratio of two fluctuation components, a slab component with parallel wavenumbers and a two-dimensional (2D) component with perpendicular wavenumbers. We perform computer simulations mostly for 80% 2D and 20% slab energy and a fluctuation amplitude on the order of B_0. The nonlinear guiding center (NLGC) theory provides a reasonable description of asymptotic perpendicular diffusion as a function of the nonaxisymmetry and particle energy. These values are roughly proportional to the particle speed times the field line diffusion coefficient, with a prefactor that is much lower than in the classical field line random walk model of particle diffusion. NLGC predicts a prefactor in closer agreement with simulations. Next we consider extreme fluctuation anisotropy and the approach to reduced dimensionality. For 99% slab fluctuation energy, field line trajectories are diffusive, but the particle motion is subdiffusive. For 99% 2D fluctuation energy, both field lines and particle motions are initially subdiffusive and then diffusive, but NLGC gives unreliable results. The time dependence of the running particle diffusion coefficient shows that in all cases asymptotic diffusion is preceded by free streaming and subdiffusion, but the latter differs from standard compound subdiffusion. We can model the time profiles in terms of a decaying negative correlation of the perpendicular velocity due to the possibility of backtracking along magnetic field lines.

Subject headings: diffusion — magnetic fields — turbulence

1. INTRODUCTION

The transport of energetic charged particles in a tenuous plasma is dominated by gyration about a local magnetic field line. Astrophysical plasmas are typically turbulent, so the field lines themselves undergo a random walk in space (Jokipii 1966). The classical field line random walk (FLRW) model of particle diffusion perpendicular to the mean field direction (say, z) assumes that a particle follows a magnetic field line with a constant parallel velocity v_z (see Fig. 1*a*). Then the particle motion in, say, x is diffusive, i.e., $\langle \Delta x^2 \rangle = 2\kappa_{xx}\Delta t$, for a particle diffusion coefficient κ_{xx} of $(1/2)vD_x$, where v is the particle speed and D_x is the field line diffusion coefficient (Jokipii 1966; Jokipii & Parker 1968). Although this is a commonly used model of particle transport, it really should apply only to "first diffusion," before the particle experiences substantial pitch-angle scattering, i.e., random changes in the parallel velocity v_z. Such parallel scattering might cause the particle to backtrack along a path nearly opposite to the preceding path (Fig. 1*b*). If the particle gyrocenter were strictly tied to one field line, this process would lead to "compound" transport, which we call compound subdiffusion, a specific type of subdiffusion with $\langle \Delta x^2 \rangle \propto (\Delta t)^{1/2}$ (Getmantsev 1963; Urch 1977; Kóta & Jokipii 2000).

In computer simulations of particle motion in a constant magnetic field with random (turbulent) fluctuations, subdiffusion is indeed found (Qin et al. 2002a; Zimbardo et al. 2006). However, when the magnetic turbulence has a strong transverse structure, the particle transport becomes diffusive again at later times (Skilling et al. 1974; Rechester & Rosenbluth 1978; Chandran & Cowley 1998; Qin et al. 2002b); see Figure 1*c*. The nonlinear guiding center (NLGC) theory has been proposed (Matthaeus et al. 2003) to derive perpendicular diffusion coefficients for this asymptotic diffusion regime, sometimes called "second diffusion."

The NLGC and FLRW theories have been compared and tested by means of computer simulations of asymptotic diffusion as a function of particle energy, as have further theories derived from NLGC. Such comparison work has considered magnetic fluctuations that are axisymmetric, i.e., with statistical properties that are invariant under rotations about the mean field axis. Stawicki (2005) pointed out that by considering nonaxisymmetric fluctuations, theories of the perpendicular diffusion of particles can be tested more rigorously. In particular, he proposed a strongly nonlinear (SNL) theory with markedly different predictions for κ_{xx}/κ_{yy}. In the present work, we examine the nonaxisymmetric case, building on our previous work on the field line random walk to now examine ensemble average statistics of the perpendicular transport of particles.

In addition to this theoretical motivation to examine the nonaxisymmetric case, there is a more practical motivation regarding the transport of energetic particles (cosmic rays) in the heliosphere. Classic measurements in the inner solar system indicated a roughly 4:3 ratio of solar wind fluctuation energy in the $\hat{\boldsymbol{z}} \times \hat{\boldsymbol{r}}$ direction relative to the orthogonal direction (Belcher & Davis 1971). Saur & Bieber (1999) inferred that the solar wind near Earth has a two-dimensional (2D) turbulence component that is symmetric with respect to the mean field, while another component has wavevectors along the radial direction. Since the mean interplanetary magnetic field is not radial but rather follows an Archimedean spiral (Parker 1958), that implies nonaxisymmetry with respect to the mean field.

Modern studies also suggest a possible role of nonaxisymmetric fluctuations in enhanced latitudinal transport of cosmic rays at high heliographic latitudes (Jokipii et al. 1995; Burger & Hattingh 1998). Note that the Archimedean spiral magnetic field in the outer heliosphere is mainly in the azimuthal direction, so

[1] Department of Physics, Faculty of Science, Mahidol University, Bangkok 10400, Thailand; ruffolo.physics@gmail.com, pattyphys@yahoo.com.
[2] Bartol Research Institute and Department of Physics and Astronomy, University of Delaware, Newark, DE 19716; paeng@bartol.udel.edu, jacominnie@yahoo.com, jwbieber@bartol.udel.edu, yswhm@bartol.udel.edu.

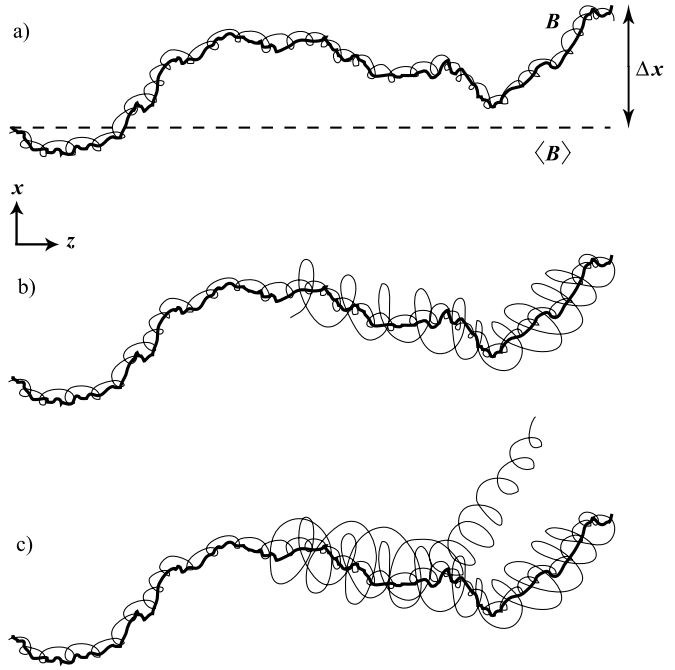

FIG. 1.—Illustration of perpendicular transport processes of particles in random magnetic fields. Thick lines indicate field lines and thin lines indicate particle trajectories; z is along the mean field and x is a perpendicular direction. (*a*) At short times, the particle gyrocenter undergoes free streaming, with $\langle \Delta x^2 \rangle \propto \Delta t^2$. Next, the gyrocenter may follow the field line random walk before the onset of substantial parallel scattering, which would yield a diffusive process ($\langle \Delta x^2 \rangle \propto \Delta t$), sometimes called "first diffusion." (*b*) Under typical solar wind conditions, parallel scattering curtails the above process, sometimes causing the particle to backtrack along the same field line. If the particle gyrocenter were strictly tied to one field line, this process would be compound subdiffusion with $\langle \Delta x^2 \rangle \propto \Delta t^{1/2}$. In our computer simulations, the particle trajectories are found to deviate from field lines, and the backtracking effect is instead manifest in a transient subdiffusive regime. (*c*) After a sufficiently long time, the particle trajectory deviates substantially from the field line; i.e., the particles follow field lines locally but not globally. This is the asymptotic diffusion regime (sometimes called "second diffusion"), confirmed by simulations and described by the nonlinear guiding center (NLGC) theory.

the two perpendicular coordinates are r and θ. However, the mean solar wind flow is essentially radial with a small deceleration, so the solar wind plasma is greatly stretched in θ with a slight compression in r. By itself, such stretching of solar wind plasma gives $b_\theta/b_r \sim r/R$, where $R = v_{\rm sw}/(\Omega \sin\theta)$ is the characteristic length of the Archimedean spiral, $v_{\rm sw}$ is the solar wind speed, and Ω is the angular frequency of solar rotation. Since R is lowest near the ecliptic plane, where it has a value of $\approx$1 AU, in the outer heliosphere, up to $r \sim 100$ AU, the stretching of solar wind plasma could generate a nonaxisymmetry of order 100. On the other hand, there could be substantial transfer of fluctuation energy between the two perpendicular directions due to dynamical couplings, which would reduce the nonaxisymmetry. In any case, one might expect substantial nonaxisymmetry of magnetic turbulence in the outer heliosphere (Jokipii 1973), and such effects are particularly relevant in the new era of measurements of Galactic and anomalous cosmic rays near and beyond the heliospheric termination shock (Stone et al. 2005).

In the present work, we extend the simulation of particle transport and the comparison with predictions of FLRW and NLGC theories in three further "directions": anisotropy, nonaxisymmetry, and time. We examine the dependence on anisotropy in the context of a two-component model of magnetic fluctuations, motivated by observations of the solar wind (Matthaeus et al. 1990), involving wavenumbers either parallel (slab component) or perpendicular (2D component) to the mean field. Observations of particle transport and solar wind fluctuations are consistent with an energy ratio of roughly 80% 2D and 20% slab turbulent energy in the inertial range (Bieber et al. 1994, 1996), although variations of this symmetry have been reported at different scales (Saur & Bieber 1999) and for varying wind speeds (Dasso et al. 2005). Gray et al. (1996) examined the field line random walk, confirming the nonperturbative theory of Matthaeus et al. (1995) for slab fractions of 0.1 to 0.99. Here we examine the field line random walk and particle transport for slab fractions from 0.01 to 0.99. In terms of nonaxisymmetry, we use the framework of Ruffolo et al. (2006) to perform simulations and compare with predictions of FLRW, NLGC, and SNL theories. Weinhorst et al. (2008) have used this framework to theoretically model perpendicular transport for a specific form of the power spectrum. We also compare our results with previous simulation work on particle transport subject to anisotropic magnetic fluctuations that employed "ellipsoidal" turbulence (Pommois et al. 2005, 2007; Zimbardo et al. 2006), which did not make specific comparisons with theoretical expectations. Finally, we examine the time history of the perpendicular transport of particles during the transient subdiffusive and asymptotic diffusive phase (when present). We find that the subdiffusion is quantitatively inconsistent with compound subdiffusion and provide a heuristic model that can explain the time dependence based on a positive term in the velocity correlation function for short-time correlations and a negative term of longer duration to account for backtracking.

2. NONLINEAR GUIDING CENTER THEORY

2.1. *Overview and Generalization to Nonaxisymmetric Fluctuations*

To understand the context of nonlinear guiding center (NLGC) theory, we consider various possible regimes of particle transport perpendicular to the mean magnetic field, as illustrated in Figure 1. Any realistic field line random walk begins with free streaming, where the field line is approximately straight because it has not yet traversed a mean free path for directional changes. The corresponding feature of particle motion is that over short distances and times, the particle trajectory is a helix around that field line at roughly constant pitch angle, the angle between the particle momentum and the magnetic field direction. Averaging over the gyration, the particle's guiding center approximately follows the field lines, which are straight over such short distances. For an ensemble of such straight line motions, the gyrocenter exhibits $\langle \Delta x^2 \rangle \propto \Delta t^2$.

The next stage is that the field line begins a random walk, which in most cases is diffusive if the ensemble is defined properly. The FLRW model of particle diffusion perpendicular to the mean field direction (Jokipii & Parker 1968) assumes that a particle follows a magnetic field line with a constant pitch angle and constant velocity v_z (Fig. 1*a*). If the field line motion in a perpendicular direction, say, x, as a function of distance z parallel to the mean field is diffusive with $\langle \Delta x^2 \rangle = 2D_x \Delta z$ for a diffusion coefficient D_x, then the FLRW model yields

$$\langle \Delta x^2 \rangle = 2D_x \langle |\Delta z| \rangle = 2\langle |v_z| \rangle D_x \Delta t = 2\kappa_{xx} \Delta t, \qquad (1)$$

where the particle diffusion coefficient is

$$\kappa_{xx} = \langle |v_z| \rangle D_x = \frac{1}{2} v D_x, \qquad (2)$$

assuming an isotropic particle distribution. This process has been called "first diffusion."

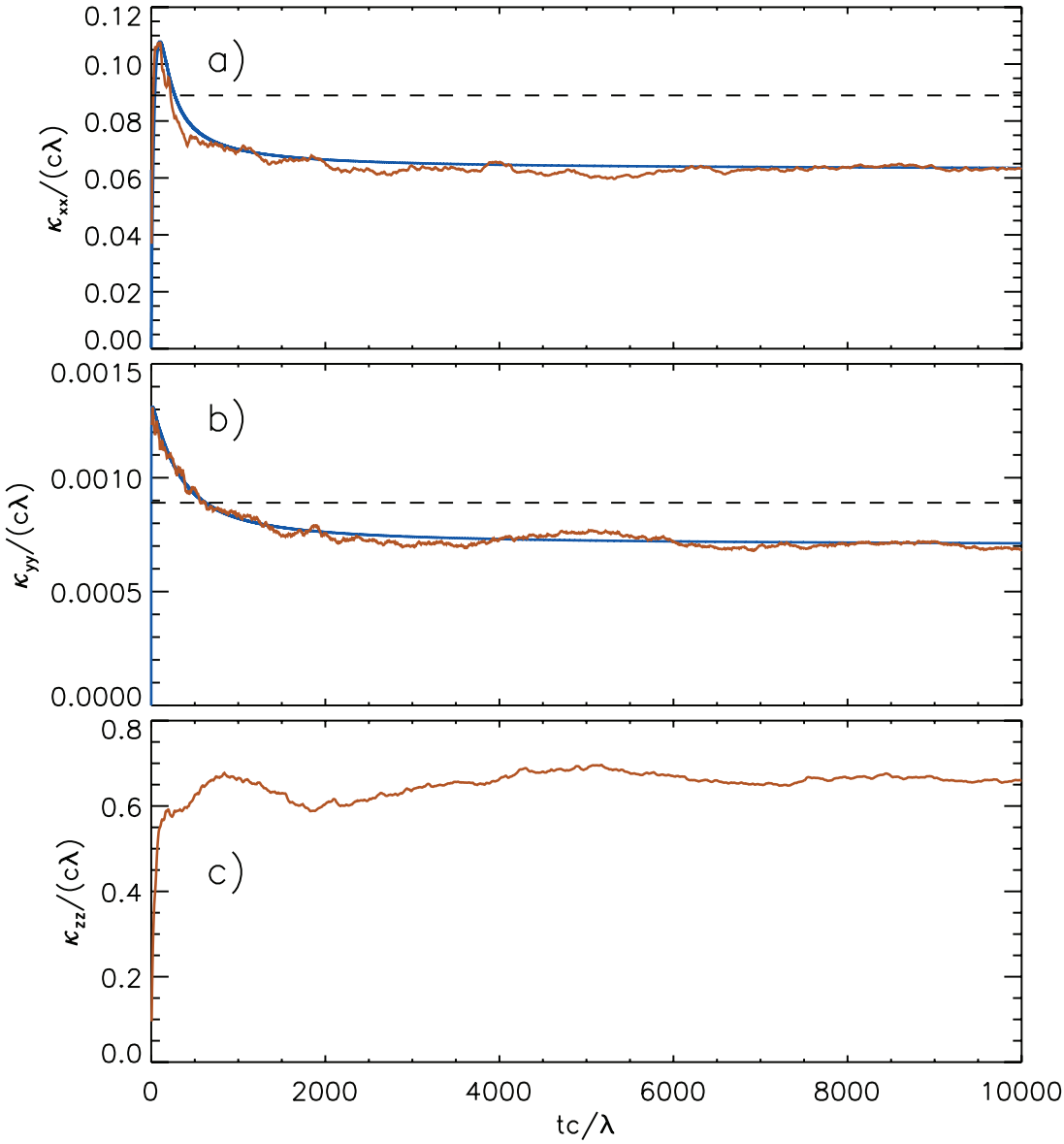

FIG. 2.—Example of running particle diffusion coefficients (*a*) κ_{xx}, (*b*) κ_{yy}, and (*c*) κ_{zz} as a function of time from computer simulations (run 3; *red lines*) and a heuristic model fit (*blue lines*). The dashed lines indicate predictions from NLGC theory for the late-time asymptotic values of κ_{xx} and κ_{yy}.

However, in practice the above process is quickly curtailed by parallel scattering, which is dominated by a resonant interaction between Alfvénic (slab) field fluctuations and the particle gyration, leading to a random walk of μ with time (Jokipii 1966). In fact, for the wide range of simulation parameters used in the present study, we do not find any time ranges with steady "first diffusive" behavior, nor is such behavior evident in other recent studies (e.g., Qin et al. 2002a, 2002b). For example, in Figure 2, the running diffusion coefficient $\kappa_{xx} \equiv \langle \Delta x^2 \rangle / (2\Delta t)$ rapidly increases and peaks, after which it immediately falls again. An increase in the running diffusion coefficient indicates that $\langle \Delta x^2 \rangle$ increases faster than $O(\Delta t)$, i.e., superdiffusion (in this case, free streaming). After the peak, the running diffusion coefficient decreases, indicating that $\langle \Delta x^2 \rangle$ increases more slowly than $O(\Delta t)$, i.e., subdiffusion. A nearly flat region indicates a diffusive regime, with $\langle \Delta x^2 \rangle \propto \Delta t$. There is no stable, flat region corresponding to first diffusion after the free streaming regime of κ_{xx} or κ_{yy}. Instead, diffusion is found as an asymptotic (late-time) state in all three panels of Figure 2.

The transient subdiffusive behavior in Figure 2 arises because the parallel scattering can cause the particle to backtrack along the same field line (Fig. 1*b*). If the particle gyrocenter were strictly tied to one field line, this process would be the so-called compound transport or compound subdiffusion, a specific form of subdiffusion (Getmantsev 1963; Urch 1977; Kóta & Jokipii 2000). In this model, $\langle \Delta x^2 \rangle \propto \Delta z$ and $\langle \Delta z^2 \rangle \propto \Delta t$, so $\langle \Delta x^2 \rangle \propto (\Delta t)^{1/2}$, and $\kappa_{xx} \propto (\Delta t)^{-1/2}$. In our computer simulations, the particle trajectories are found to deviate from field lines, and the backtracking effect is instead manifest in a transient subdiffusive regime, with κ_{xx} and κ_{yy} decreasing more slowly with time. Note that at these intermediate time and distance scales, the turbulent field line random walk and particle transport from a localized "injection region" also exhibit interesting spatial structures in the perpendicular directions (Giacalone et al. 2000; Ruffolo et al. 2003; Zimbardo et al. 2004; Pommois et al. 2005; Chuychai et al. 2007) that are characteristic of percolative phenomena (Rechester & Rosenbluth 1978; Isichenko 1991).

Finally at late times, when using a turbulence model with substantial fluctuation energy at both parallel and perpendicular wavevectors as is typically observed in space plasmas (see § 2.2), the particle motion is again diffusive (so-called second diffusion),

because particles are not tied to a single field line (Fig. 1*c*). According to Qin et al. (2002b), "transverse complexity" of the magnetic turbulence is required for the recovery of diffusion.

Matthaeus et al. (2003) presented the original NLGC theory to determine the coefficient of perpendicular diffusion κ_{xx} at late times, for axisymmetric, homogeneous fluctuations. (Because of axisymmetry, $\kappa_{yy} = \kappa_{xx}$.) The NLGC theory aims to explain motion in the perpendicular directions x and y as a function of time, using the Taylor-Green-Kubo formula (e.g., Kubo 1957) for velocity decorrelation. Consider a velocity component v_x of the guiding center of the particle gyromotion, which is guided by the local magnetic field direction b_x,

$$v_x = a v_z b_x / B_0. \tag{3}$$

Then $v_x(t)$ is taken to decorrelate over time according to two independent processes: the decorrelation of v_z (parallel scattering) and of b_x (the field line random walk). These determine the random flights of x and y in a statistical sense.

With the further assumptions of statistical homogeneity, Corrsin's independence hypothesis (Corrsin 1959), and diffusive spreading, Matthaeus et al. (2003) used the Taylor-Green-Kubo formalism to derive the implicit equation

$$\kappa_{xx} = \frac{a^2 v^2}{3B_0^2} \int \frac{S_{xx}(\boldsymbol{k}) d^3k}{v/\lambda_\parallel + \left(k_x^2 + k_y^2\right)\kappa_{xx} + k_z^2 \kappa_{zz} + \gamma(\boldsymbol{k})}, \tag{4}$$

where $a = 1/\sqrt{3}$, B_0 is the mean field, in the z-direction, $S_{xx}(\boldsymbol{k})$ is a power spectrum defined as the Fourier transform of the correlation function $R_{xx}(\boldsymbol{r}) \equiv \langle b_x(0) b_x(\boldsymbol{r})\rangle$, $\lambda_\parallel = 3\kappa_{zz}/v$ is the mean free path of parallel scattering, and $\gamma(\boldsymbol{k})$ is the rate of temporal decorrelation of the turbulence.

With a straightforward generalization of equation (4) to nonaxisymmetric fluctuations, we obtain the coupled equations

$$\kappa_{xx} = \frac{a^2 v^2}{3B_0^2} \int \frac{S_{xx}(\boldsymbol{k}) d^3k}{v/\lambda_\parallel + k_x^2 \kappa_{xx} + k_y^2 \kappa_{yy} + k_z^2 \kappa_{zz} + \gamma(\boldsymbol{k})},$$
$$\kappa_{yy} = \frac{a^2 v^2}{3B_0^2} \int \frac{S_{yy}(\boldsymbol{k}) d^3k}{v/\lambda_\parallel + k_x^2 \kappa_{xx} + k_y^2 \kappa_{yy} + k_z^2 \kappa_{zz} + \gamma(\boldsymbol{k})}, \tag{5}$$

where the coefficient a is taken to be the same for the x- and y-motion. Note that these equations require an input of κ_{zz} (which in turn sets $\lambda_\parallel$), typically from direct computer simulations. Here we set $\gamma = 0$ for simplicity, neglecting any dynamics of the magnetic fields over the time sampled by the energetic particle motion.

Although NLGC takes parallel scattering into account, it does not track the parallel motion along z and does not consider the process of backtracking along the same field line. This, along with the assumption of diffusive spreading, is why NLGC applies only to asymptotic diffusion and not to the preceding subdiffusive range. At late times, the backtracking is subsumed into the general diffusion process, with limited time periods of anticorrelated forward and backward flights—in a random direction—contributing to the general milieu of random flights in all directions. The time history of the perpendicular transport will be addressed in detail in § 4.

As an alternative to NLGC, Stawicki (2005) derived a strongly nonlinear (SNL) theory, envisioned to apply for strong magnetic fluctuations. In contrast with NLGC theory, which models the guiding center velocity, SNL aims to treat the instantaneous particle velocity. A key assumption is that the random walk in velocity space restarts at zero before every time step τ in the random walk (going from eqs. [5]–[6] to eqs. [7]–[8] in Stawicki 2005). Here we note that for static magnetic fluctuations, which do no work on the particle, the particle speed v is fixed by the initial condition. Thus, in actuality the particle velocity is constrained to a shell of radius v, and it is unrealistic that each "step" in the velocity space random walk proceeds from $\boldsymbol{v} = 0$.

Stawicki (2005) suggested that simulations of particle motion in nonaxisymmetric fluctuations could distinguish between the predictions of NLGC and SNL, thus providing part of the motivation for the present study. He pointed out that SNL was not complete in the sense that there is no specification of the parameters a_x and a_y (analogous to a in NLGC theory). Thus, we cannot examine SNL predictions for κ_{xx} or κ_{yy}, or verify that the equations have a solution for cases of interest. However, if SNL solutions exist, and if we assume that $a_x = a_y$ (as we assume for NLGC), then $(\kappa_{xx}/\kappa_{yy})_{\rm SNL} = 1/(\kappa_{xx}/\kappa_{yy})_{\rm NLGC}$. This inversion of the ratio would be a very noticeable effect, allowing us to clearly test the SNL prediction for nonaxisymmetric fluctuations (§ 3).

Finally, we note that various works in the literature have presented additions or modifications to NLGC theory, which can improve on its assumptions and/or accuracy. The original NLGC theory views the parallel diffusion coefficient κ_{zz} as an "input" that the "user" of NLGC must know by other means. To test NLGC theory in and of itself, one can use κ_{zz} as determined by test particle simulations (as in the present work). For a purely theoretical approach, one could use the classic quasilinear theory of parallel diffusion, taking into account the small fraction ($\sim$20%) of solar wind turbulence that is slablike (Alfvénic). Further steps were to consider dynamical turbulence (Bieber et al. 1994) as input to NLGC theory (Bieber et al. 2004; Shalchi et al. 2004a), and the nonlinear anisotropic dynamical turbulence model of parallel diffusion to provide such input (Shalchi et al. 2006). NLGC theory itself is modified by Shalchi (2006) and Shalchi & Kourakis (2007). Furthermore, it is appealing to merge the theories of parallel and perpendicular diffusion, as in weakly nonlinear theory (Shalchi et al. 2004b), but the combined theory is very complicated (see also le Roux & Webb 2007). A somewhat less complicated merger was proposed by Qin (2007).

Nevertheless, in the present work we start from the original form of NLGC because of its simplicity and generality, e.g., that it allows a general form of the power spectrum. Note also that Bieber et al. (2004) have successfully used the original NLGC theory, with "input" parallel diffusion coefficients from dynamical turbulence theory that closely match coefficients inferred by observations, to explain measurements of Jovian electrons and their spread away from the Sun-Jupiter field line, as well as the energy dependence of the Galactic cosmic-ray latitude gradient determined from the *Ulysses* mission. Minnie et al. (2005) also found that, when used in an ab initio cosmic-ray modulation model, NLGC was more consistent with latitudinal gradients measured by *Ulysses* than a previous theory by Bieber & Matthaeus (1997). Here we aim to learn about concepts of perpendicular transport, and thus, we examine NLGC theory using the simulated value of κ_{zz} as input, without using a theory of parallel diffusion.

2.2. *Two-Component Model of Nonaxisymmetric Fluctuations*

The two-component model was developed in response to the observation that magnetic fluctuations in the solar wind include modes that have both parallel and perpendicular wavevector components relative to the mean magnetic field (Matthaeus et al.

1990). The two-component model is a simple way to achieve this. This model assumes that

$$\boldsymbol{B} = \boldsymbol{B}_0 + \boldsymbol{b}(x, y, z), \tag{6}$$

where the mean field $\boldsymbol{B}_0 = B_0\hat{\boldsymbol{z}}$ is constant. The static fluctuating field is taken to have two components,

$$\boldsymbol{b} = \boldsymbol{b}^{\rm 2D}(x, y) + \boldsymbol{b}^{\rm slab}(z). \tag{7}$$

The two-component model has been shown to provide a useful description of solar wind fluctuations (Bieber et al. 1996) and the parallel transport of particles in interplanetary space (Bieber et al. 1994).

In Fourier space, the slab component has only parallel wavevectors (along the k_z-axis) and the 2D component has only perpendicular wavevectors (in the k_x-k_y plane). This is a great simplification for both analytic calculations and for computer simulations, in which a general 3D Fourier transform is replaced with 1D and 2D transforms, yet the summed fluctuation still varies in all three dimensions. Each fluctuation component has $\boldsymbol{b}$ perpendicular to $\hat{\boldsymbol{z}}$ with $\langle \boldsymbol{b} \rangle = 0$. For brevity, we refer to $\langle b^2 \rangle$ as the magnetic energy of the fluctuations and define $b \equiv (\langle b^2 \rangle)^{1/2}$, either for the total fluctuation or for individual components.

A special concern for magnetic fluctuations is that the divergence must be zero. The mean and slab fields explicitly satisfy this condition, and thus, the slab fluctuations in different directions, $b_x(z)$ and $b_y(z)$, can be specified independently. To obtain a nonaxisymmetric slab field, we can simply set the correlation length, ℓ_c, and/or the rms slab magnitude, $b^{\rm slab}$, to be different for fluctuations in the x- and y-directions. In later sections of the present work, we maintain the same correlation lengths, but vary the ratio of magnitudes, $\eta = b_x^{\rm slab}/b_y^{\rm slab}$.

For 2D fluctuations, the magnetic field components are not independent, because we require $\partial b_x/\partial x + \partial b_y/\partial y = 0$. Thus, it is useful to specify a potential function $a(x, y)$ so that

$$\boldsymbol{b}^{\rm 2D}(x, y) = \nabla \times [a(x, y)\hat{\boldsymbol{z}}]. \tag{8}$$

Note that $\boldsymbol{b}^{\rm 2D} \perp \nabla a$, so $\boldsymbol{b}$ follows contours of constant $a(x, y)$. Here $a(x, y)$ can be taken to be a random function fluctuating about a mean value of zero, with a well-behaved power spectrum $A(k_x, k_y)$ (Ruffolo et al. 2004). Then the power spectra of field components are given by $S_{xx}^{\rm 2D} = k_y^2 A$ and $S_{yy}^{\rm 2D} = k_x^2 A$. These and other properties of 2D magnetic fluctuations have been summarized by Matthaeus et al. (2007).

For the axisymmetric case, $A(k_x, k_y)$ is constant along circles of constant $k_\perp = (k_x^2 + k_y^2)^{1/2}$ in (k_x, k_y)-space, so $A = A(k_\perp)$. We model nonaxisymmetric cases by taking $A(k_x, k_y)$ to be constant along ellipses in (k_x, k_y)-space that have a k_y-to-k_x aspect ratio of ξ, the ellipticity parameter (Ruffolo et al. 2006). In terms of the "stretched" coordinates $k_x' = \xi^{1/2}k_x$, $k_y' = \xi^{-1/2}k_y$, and $k_\perp' = (k_x'^2 + k_y'^2)^{1/2}$, we now have $A = A(k_\perp')$. The spatial structures are similarly stretched, with a statistical x-to-y aspect ratio of ξ.

In summary, our model incorporates two types of nonaxisymmetry: (1) a difference between the two "polarizations" of the slab component, characterized by η, and (2) a stretching of the 2D potential function, characterized by ξ. In later sections of the present work, we use $\xi = \eta$ for simplicity. Then the ratio of rms amplitudes is $b_x/b_y = \xi = \eta$ for the 2D and slab components individually and for the combined field, so we also refer to the nonaxisymmetry as b_x/b_y.

Previous work has examined the diffusion coefficients D_x and D_y of the magnetic FLRW (Ruffolo et al. 2006), defined in terms of mean squared displacements as a function of distance Δz along the mean field,

$$D_x = \frac{\langle (\Delta x)^2 \rangle}{2\Delta z}, \quad D_y = \frac{\langle (\Delta y)^2 \rangle}{2\Delta z}. \tag{9}$$

With assumptions of homogeneity, Corrsin's independence hypothesis, and a diffusive process, those authors derived coupled equations for D_x and D_y in terms of the power spectra of the fluctuations. For the two-component model with $\xi = \eta$, the equations for D_x and D_y decouple and have analytic solutions,

$$D_x = \frac{1}{2}\left[D_x^{\rm slab} + \sqrt{\left(D_x^{\rm slab}\right)^2 + 2\frac{b_x^2}{b_y^2}I}\right],$$
$$D_y = \frac{1}{2}\left[D_y^{\rm slab} + \sqrt{\left(D_y^{\rm slab}\right)^2 + 2\frac{b_y^2}{b_x^2}I}\right], \tag{10}$$

in terms of

$$D_i^{\rm slab} = \frac{\langle b_i^2 \rangle^{\rm slab}}{B_0^2}\ell_c, \tag{11}$$

for $i = x, y$, and

$$I = \langle a^2 \rangle / B_0^2, \tag{12}$$

which are in turn related to the power spectra of slab magnetic fields and the 2D potential function, respectively. The above equations correspond to the result of Matthaeus et al. (1995) as applied individually to D_x and D_y.

For two-component fluctuations, the coupled equations for nonaxisymmetric NLGC (eqs. [5]) become

$$\kappa_{xx} = \frac{a^2v^2}{3B_0^2}\int \frac{S_{xx}^{\rm 2D}(k_x, k_y)d^2k}{v/\lambda_\parallel + k_x^2\kappa_{xx} + k_y^2\kappa_{yy}} + \frac{a^2v^2}{3B_0^2}\int \frac{S_{xx}^{\rm slab}(k_z)dk_z}{v/\lambda_\parallel + k_z^2\kappa_{zz}},$$
$$\kappa_{yy} = \frac{a^2v^2}{3B_0^2}\int \frac{S_{yy}^{\rm 2D}(k_x, k_y)d^2k}{v/\lambda_\parallel + k_x^2\kappa_{xx} + k_y^2\kappa_{yy}} + \frac{a^2v^2}{3B_0^2}\int \frac{S_{yy}^{\rm slab}(k_z)dk_z}{v/\lambda_\parallel + k_z^2\kappa_{zz}}. \tag{13}$$

The final terms in these two equations can be called $\kappa_{xx}^{\rm slab}$ and $\kappa_{yy}^{\rm slab}$, respectively. The assumption $\xi = \eta$ in our formulation of nonaxisymmetric two-component fluctuations again allows the two equations to be decoupled. Equations (13) imply that the ratios κ_{xx}/κ_{yy}, $\kappa_{xx}^{\rm slab}/\kappa_{yy}^{\rm slab}$, D_x/D_y, and $(b_x/b_y)^2$ are all equal to ξ^2. Mathematically, the problem is isotropic in the "stretched" coordinates $k_x' = \xi^{1/2}k_x$ and $k_y' = \xi^{-1/2}k_y$, so the above ratios are all unity in those coordinates and scale in the same way when transforming back to (k_x, k_y). The decoupled equations (13) give

$$\kappa_g - \kappa_g^{\rm slab} = \frac{1}{2}\frac{a^2v^2}{3B_0^2}\int \frac{k_\perp'^2 A(k_\perp')d^2k'}{v/\lambda_\parallel + \kappa_g k_\perp'^2} \tag{14}$$

in terms of the geometric means $\kappa_g \equiv (\kappa_{xx}\kappa_{yy})^{1/2}$ and $\kappa_g^{\rm slab} \equiv (\kappa_{xx}^{\rm slab}\kappa_{yy}^{\rm slab})^{1/2}$, from which one can determine $\kappa_{xx} = (b_x/b_y)\kappa_g$ and $\kappa_{yy} = (b_y/b_x)\kappa_g$.

2.3. *Limit of Weak Parallel Scattering*

It is instructive to examine the NLGC results for κ_{xx} and κ_{yy} by solving equation (14) in the limit where $\lambda_\parallel$ is long, i.e., for weak parallel scattering. See Minnie et al. (2008) for a related derivation in the axisymmetric case. Interestingly, the result is slightly different from the classic FLRW result of $\kappa = (1/2)vD$ for first diffusion (see § 1 and Fig. 1*a*), in which parallel scattering is completely neglected and particles strictly (globally) follow field lines. This is because NLGC theory addresses an asymptotic perpendicular diffusion regime (Fig. 1*c*), in which the particle motion is guided by the local field line direction in a statistical sense, but is not strictly tied to an individual field line. By taking parallel scattering to be weak but not completely neglected, one obtains $\kappa \propto vD$ with a prefactor that depends on the rms value of v_z. In other words, the classic FLRW formula, with a different numerical prefactor, can provide a good description of asymptotic diffusion in the weak scattering limit, because perpendicular excursions of particles are statistically related to perpendicular excursions of field lines. In § 3, we find that for parameters that might be expected for energetic particles in the heliosphere, simulation and NLGC results for κ are reasonably well organized by vD, even though $\lambda_\parallel$ is not particularly long.

First, we note that if we do not assume $\xi = \eta$ in our model of nonaxisymmetry, the limit of long $\lambda_\parallel$ yields

$$\left(K_{xx} - K_{xx}^{\rm slab}\right)\left(K_{yy} + \frac{\sqrt{K_{xx}K_{yy}}}{\xi}\right) = I,$$
$$\left(K_{yy} - K_{yy}^{\rm slab}\right)\left(K_{xx} + \xi\sqrt{K_{xx}K_{yy}}\right) = I, \quad (15)$$

where all quantities κ are scaled as $K_{ii} \equiv \sqrt{3}\kappa_{ii}/(av)$, and we have $K_{ii}^{\rm slab} = aD_i^{\rm slab}$ for $i = x, y$. This is in direct analogy to the coupled equations for the field line diffusion coefficients,

$$\left(D_x - D_x^{\rm slab}\right)\left(D_y + \frac{\sqrt{D_xD_y}}{\xi}\right) = I,$$
$$\left(D_y - D_y^{\rm slab}\right)\left(D_x + \xi\sqrt{D_xD_y}\right) = I, \quad (16)$$

as derived by Ruffolo et al. (2006), and the various limits considered in that work are mathematically valid for K_{ii}.

Further physical insight can be gained for the case of equal nonaxisymmetry in the slab and 2D components of turbulence, with $\xi = \eta = b_x/b_y$, for which the equations decouple as described in § 2.2. To find the solution of equation (14) in the limit of long $\lambda_\parallel$, let us first consider the slab term $\kappa_g^{\rm slab} = (\kappa_{xx}^{\rm slab}\kappa_{yy}^{\rm slab})^{1/2}$. Using $\kappa_{zz} = v\lambda_\parallel/3$, we have

$$\kappa_{xx}^{\rm slab} \equiv \frac{a^2v^2}{3B_0^2}\int \frac{S_{xx}^{\rm slab}(k_z)dk_z}{v/\lambda_\parallel + k_z^2\kappa_{zz}} = \frac{a^2v\lambda_\parallel}{3B_0^2}\int \frac{S_{xx}^{\rm slab}(k_z)dk_z}{1+\lambda_\parallel^2k_z^2/3}. \quad (17)$$

Now suppose the scattering is weak, so that $\lambda_\parallel$ is much greater than the parallel coherence (bendover) scale of the turbulence, λ. Then the factor $1/(1+\lambda_\parallel^2k_z^2/3)$ selects k_z values very close to zero, and if $S_{xx}^{\rm slab}(0)$ is finite, then we obtain

$$\kappa_{xx}^{\rm slab} = \frac{a^2v\lambda_\parallel S_{xx}^{\rm slab}(0)}{3B_0^2}\int \frac{dk_z}{1+\lambda_\parallel^2k_z^2/3} = \frac{\pi a^2vS_{xx}^{\rm slab}(0)}{\sqrt{3}B_0^2}. \quad (18)$$

Note that the field line diffusion coefficient for slab turbulence (Jokipii 1966; Jokipii & Parker 1968) is given (in the present notation) by

$$D_x^{\rm slab} = \frac{\pi S_{xx}^{\rm slab}(0)}{B_0^2}. \quad (19)$$

Thus, the limit of long $\lambda_\parallel$ yields

$$\kappa_{xx}^{\rm slab} = \frac{a^2}{\sqrt{3}}vD_x^{\rm slab}. \quad (20)$$

Similarly, one can show that

$$\kappa_{yy}^{\rm slab} = \frac{a^2}{\sqrt{3}}vD_y^{\rm slab}, \quad (21)$$

$$\kappa_g^{\rm slab} = \frac{a^2}{\sqrt{3}}v\sqrt{D_x^{\rm slab}D_y^{\rm slab}}. \quad (22)$$

Now let us examine the 2D term on the right-hand side of equation (14). In the limit of long $\lambda_\parallel$, the $(v/\lambda_\parallel)$ term can be neglected. (To be precise, the criterion is that $\lambda_\parallel \gg v\ell_\perp^2/\kappa_g$, where $\ell_\perp = 1/k'_{0\perp}$ is the coherence [bendover] scale of the 2D turbulence. The integrand is only significant over the region $k' \lesssim k'_{0\perp}$, and with this criterion, the $v/\lambda_\parallel$ term is important over a negligible portion of that region.) Neglecting this term yields

$$\kappa_g - \kappa_g^{\rm slab} = \frac{1}{2}\frac{a^2v^2}{3B_0^2}\frac{1}{\kappa_g}\int A(k_\perp)d^2k, \quad (23)$$

where we have used the relation $d^2k = d^2k'$. Now we make use of the ultrascale of a 2D fluctuating field,

$$\tilde{\lambda} \equiv \sqrt{\frac{\int A(k_\perp)d^2k}{\langle b^2\rangle^{\rm 2D}}} = \sqrt{\frac{\langle a^2\rangle}{\langle b^2\rangle^{\rm 2D}}}, \quad (24)$$

a length scale that arises in the theory of field line random walk. The original definition of the ultrascale (Matthaeus et al. 1995) was different by a factor of $1/\sqrt{2}$; here we follow the definition of Ruffolo et al. (2004) and Matthaeus et al. (2007). Its relevance to NLGC theory is also pointed out by Minnie et al. (2008). Matthaeus et al. (2007) have expanded on its properties, including situations in which it is finite or divergent, and an example of how the ultrascale and correlation scale are independent quantities for a power spectrum of sufficient mathematical or physical complexity. For many turbulent 2D spectra of astrophysical interest, the ultrascale is finite.

We then have

$$\kappa_g - \kappa_g^{\rm slab} = \frac{1}{2}\frac{a^2v^2}{3B_0^2}\frac{1}{\kappa_g}\tilde{\lambda}^2\langle b^2\rangle^{\rm 2D}. \quad (25)$$

We note a similarity with the field line diffusion coefficient for the 2D component of turbulence (Matthaeus et al. 1995; Ruffolo et al. 2004),

$$D_\perp^{\rm 2D} = \frac{\tilde{\lambda}}{\sqrt{2}}\frac{b^{\rm 2D}}{B_0}. \quad (26)$$

In the nonaxisymmetric case, this quantity is the geometric mean of D_x^{2D} and D_y^{2D} (Ruffolo et al. 2006). We then obtain

$$\kappa_g - \kappa_g^{\rm slab} = \frac{a^2 v^2}{3} \frac{\left(D_\perp^{2D}\right)^2}{\kappa_g}, \tag{27}$$

which has the solution

$$\kappa_g = \frac{\kappa_g^{\rm slab}}{2} + \sqrt{\frac{\left(\kappa_g^{\rm slab}\right)^2}{4} + \left(\kappa_g^{2D}\right)^2}, \tag{28}$$

where

$$\kappa_g^{2D} \equiv \frac{a}{\sqrt{3}} v D_\perp^{2D} = \frac{a}{\sqrt{3}} v \sqrt{D_x^{2D} D_y^{2D}}, \tag{29}$$

which is directly analogous to equation (22) for the slab contribution, except for a different power of a. Since we are using $\xi = \eta$, all ratios of x- and y-quantities are the same, and we can also write

$$\kappa_{ii} = \frac{\kappa_{ii}^{\rm slab}}{2} + \sqrt{\frac{\left(\kappa_{ii}^{\rm slab}\right)^2}{4} + \left(\kappa_{ii}^{2D}\right)^2}, \tag{30}$$

for $i = x, y$, $\kappa_{ii}^{\rm slab} = (a^2/\sqrt{3}) v D_i^{\rm slab}$, and $\kappa_{ii}^{2D} = (a/\sqrt{3}) v D_i^{2D}$. Note that Matthaeus et al. (2003) recommend using $a = 1/\sqrt{3}$, for which we have $\kappa_{ii} = v D_i/(3\sqrt{3})$ in the slab limit and $\kappa_{ii} = v D_i/3$ in the 2D limit.

Physically, these limiting expressions can be motivated as follows. For asymptotic diffusion with a long mean free path for parallel scattering, the particle motion decorrelates (changes direction) when the magnetic field decorrelates along the particle orbit. The decorrelation time τ and the perpendicular velocity determine the diffusion coefficient in, say, the x-direction,

$$\kappa_{xx} \sim \left\langle v_x^2 \right\rangle \tau. \tag{31}$$

For slablike fluctuations, the decorrelation occurs after traveling in the z-direction on the order of the correlation length, ℓ_c. Then we have

$$\tau \sim \frac{\ell_c}{v_{z,\rm rms}}. \tag{32}$$

Using equation (3) and the v_z-b_x independence hypothesis, NLGC theory expands $\langle v_x^2 \rangle$ to give

$$\kappa_{xx}^{\rm slab} \sim a^2 \frac{\left\langle b_x^2 \right\rangle}{B_0^2} v_{z,\rm rms}^2 \frac{\ell_c}{v_{z,\rm rms}}. \tag{33}$$

Noting that in the slab case, the field line diffusion coefficient is (Jokipii & Parker 1968; see also Ruffolo et al. 2004)

$$D \sim \frac{\left\langle b_x^2 \right\rangle}{B_0^2} \ell_c, \tag{34}$$

we have

$$\kappa_{xx}^{\rm slab} \sim a^2 v_{z,\rm rms} D = \frac{a^2}{\sqrt{3}} v D. \tag{35}$$

That is indeed the limiting behavior found above.

Turning to the 2D-dominated case, the random walk decorrelates when traversing perpendicular structures on the order of the ultrascale $\tilde{\lambda}$ (Matthaeus et al. 1995), so

$$\tau \sim \frac{\tilde{\lambda}^2}{2\kappa_{xx}^{2D}}. \tag{36}$$

Then we obtain

$$\kappa_{xx}^{2D} \sim a^2 \frac{\left\langle b_x^2 \right\rangle}{B_0^2} v_{z,\rm rms}^2 \frac{\tilde{\lambda}^2}{2\kappa_{xx}^{2D}}, \tag{37}$$

$$\kappa_{xx}^{2D} \sim a \frac{\tilde{\lambda}}{\sqrt{2}} \frac{\sqrt{\left\langle b_x^2 \right\rangle}}{B_0} v_{z,\rm rms}. \tag{38}$$

For the 2D case, the field line diffusion coefficient is (Ruffolo et al. 2004)

$$D \sim \frac{\tilde{\lambda}}{\sqrt{2}} \frac{\sqrt{\left\langle b_x^2 \right\rangle}}{B_0}, \tag{39}$$

so we now obtain

$$\kappa_{xx}^{2D} \sim a v_{z,\rm rms} D = \frac{a}{\sqrt{3}} v D. \tag{40}$$

This can explain the above result for the 2D-dominated case.

In summary, in the case where $\lambda_\parallel$ is much longer than other relevant length scales, we have shown that the NLGC expressions for asymptotic perpendicular diffusion tend to $\kappa \propto vD$, like the FLRW expressions for first diffusion. The prefactors are different; the value of 1/2 for FLRW is replaced by $1/(3\sqrt{3})$ for slab-dominated up to 1/3 for 2D-dominated fluctuations for NLGC with a long $\lambda_\parallel$. The NLGC prefactor is determined by a rms parallel velocity, rather than the mean magnitude as in the FLRW model. A key point is that in NLGC theory for asymptotic diffusion (Fig. 1*c*), the particle motion is guided by the local field line direction in a statistical sense rather than in a strict global sense.

3. PARTICLE DIFFUSION COEFFICIENTS

3.1. *Numerical Methods*

This work employs two types of numerical methods to study the ensemble average statistics of energetic charged particles in a fluctuating magnetic field. We numerically evaluate the predictions of NLGC theory and perform direct computer simulations to integrate the equations of motion. In addition, to study the predictions of the FLRW model of particle motion, we need to evaluate the FLRW. Thus, for each run we also numerically evaluate the predictions of the nonperturbative theory of Ruffolo et al. (2006) for the FLRW and perform direct computer simulations of the field line trajectories.

For each run, the two coupled integral equations of NLGC theory as generalized for axisymmetric fluctuations (eq. [5]), as well as the coupled equations of Ruffolo et al. (2006) for D_x and D_y, are solved numerically using the Mathematica program (Wolfram Research, Inc.). In particular, we use "discrete" theory in which all integrals over $\boldsymbol{k}$-space are replaced by sums over the same grid points used in the computer simulations. When both the theory and simulations use the same fluctuation modes, we avoid a possible discrepancy due to different discretizations.

For computer simulations, we first construct the magnetic field in three dimensions to closely correspond with assumed power spectra, using the same techniques as Ruffolo et al. (2006). For slab fluctuations, we use

$$S_{ii}^{\rm slab}(k_z) = \frac{C_i^{\rm slab}}{\left[1+(k_z\lambda)^2\right]^{5/6}}, \quad (i=x,y), \tag{41}$$

where $C_i^{\rm slab}$ is a normalization constant of the i-component, set so as to obtain the desired slab turbulence energy $\langle b^2\rangle^{\rm slab} = f_s b^2$ and the desired ratio b_x/b_y, and λ is a parallel coherence scale that is directly related to the correlation length ℓ_c (taken to be the same for $i = x, y$). For 2D fluctuations, we specify the power spectrum $A(k_x, k_y) = A(k'_\perp)$, and as discussed in § 2.2, we then have

$$S_{xx}^{\rm 2D}(k_x,k_y) = k_y^2 A\left(k'_\perp\right), \quad S_{yy}^{\rm 2D}(k_x,k_y) = k_x^2 A\left(k'_\perp\right). \tag{42}$$

The function of A that we use is

$$A\left(k'_\perp\right) = \frac{C^{\rm 2D}}{\left[1+\left(k'_\perp\ell_\perp\right)^2\right]^{7/3}}, \tag{43}$$

where $C^{\rm 2D}$ is set to obtain the desired 2D turbulence energy $\langle b^2\rangle^{\rm 2D} = (1-f_s)b^2$. These forms of the slab and 2D power spectra are consistent with a Kolmogorov power law in the omnidirectional power spectrum at high wavenumber (Ruffolo et al. 2004), while rolling over to constant values of $S_{ii}^{\rm slab}$ and A at small wavenumbers. They provide a reasonable description of observed power spectra in interplanetary space over the energy-containing and inertial ranges of turbulence (Jokipii & Coleman 1968; Bieber et al. 1996). Note also that the spectrum in equation (43) gives rise to a finite ultrascale $\tilde{\lambda}$ of order $\ell_\perp$, as discussed by Matthaeus et al. (2007).

In the simulations, we set $\ell_\perp = \lambda$ and expressed all distances in terms of λ. The periodic box size along z was $L = 10^4$, and the 1D fast Fourier transform for slab fluctuations employed $2^{22} = 4{,}194{,}304$ grid points. Along each perpendicular direction the periodic box size was 100, and the fast Fourier transform for 2D fluctuations included 4096×4096 grid points. The input to the Fourier transforms, $b_i(\boldsymbol{k})$, had a magnitude proportional to $[S_{ii}(\boldsymbol{k})]^{1/2}$ and a random phase. The phases were independent for each distinct Fourier mode $\boldsymbol{k}$ except as constrained to obtain a real fluctuation $b_i(\boldsymbol{x})$.

To simulate field line trajectories, the field line equations

$$\frac{dx}{dz} = \frac{b_x(x,y,z)}{B_0}, \quad \frac{dy}{dz} = \frac{b_y(x,y,z)}{B_0} \tag{44}$$

were solved by a fourth-order Runge-Kutta method with adaptive step size control (Press et al. 1992). Field line trajectories were traced from random starting locations within the simulation box. Ensemble average statistics were collected in terms of the mean squared perpendicular displacements Δx^2 and Δy^2 as a function of the parallel displacement Δz, and we computed running diffusion coefficients D_x and D_y. Field line tracing was only performed over a small percentage of the parallel box length, to avoid periodicity effects.

To simulate particle trajectories, we used the same Runge-Kutta method to solve the Newton-Lorentz equations as scaled to use distances in units of λ and time in units of λ/c (Tooprakai et al. 2007),

$$\frac{d\boldsymbol{v}}{dt} = \alpha \boldsymbol{v} \times \boldsymbol{B}(\boldsymbol{x}), \tag{45}$$

where $\alpha \equiv qB_0\lambda/(\gamma mc)$ and γ is the Lorentz factor. The particles are taken to be protons. We set the mean field B_0 to 5 nT, as is typical in interplanetary space near Earth, and for almost all runs we set $b = B_0$, where b is the rms fluctuation for 2D + slab turbulence. For each run, ensemble average statistics were collected for 1000 particles that started at random locations in the simulation box, with random directions for an initially isotropic distribution. These 1000 particles comprised 10 particles each for 100 realizations of the 2D turbulence, i.e., for 100 independent sets of random phases in Fourier space. The realization of 2D turbulence was changed frequently to help ensure an adequate sampling of the wide variety of possible 2D structures for $a(x, y)$. For a given run, one slab realization was used for all particles. From the mean squared perpendicular displacements Δx^2 and Δy^2, we computed running diffusion coefficients $\kappa_{xx} \equiv \langle \Delta x^2\rangle/(2t)$ and $\kappa_{yy} \equiv \langle \Delta y^2\rangle/(2t)$ as a function of time.

We performed tests to check that the box sizes did not affect the results. For all runs, the spread in particle positions was a small percentage of the parallel box length and was not much greater than the perpendicular box size. We consider it important to avoid periodicity effects in z, because the field line random walk exactly repeats after a parallel box length. We have verified that periodicity effects are not as important in the perpendicular directions, because a field line or particle trajectory in two dimensions with periodic boundary conditions is much less likely to wander back to the same (x, y) coordinates, or within a coherence scale thereof.

3.2. *Diffusion Coefficients*

We performed 13 simulation runs to determine running particle diffusion coefficients perpendicular (κ_{xx} and κ_{yy}) and parallel (κ_{zz}) to the mean field as a function of time for varying nonaxisymmetry (b_x/b_y), particle energy (E), and anisotropy (expressed by the slab fraction of the turbulent energy, f_s). Tables 1 and 2 summarize the asymptotic diffusion coefficients in units of $c\lambda$, as well as the time duration T that was deemed necessary to measure a steady asymptotic regime. Each value reported for an asymptotic diffusion coefficient was an average over the last 1/4 of the simulation time, e.g., from $t = 7500\lambda/c$ to $10{,}000\lambda/c$ for run 3 in Figure 2. In addition, numerical values for NLGC discrete theory are presented, as are the relevant field line diffusion coefficients, both from simulations and theory. We show the ratios $\kappa_{ii}/(vD_i)$, for $i = x, y$, from simulations and NLGC theory; the value would be 0.5 in the FLRW model.

The parameter values explored in these runs are intended to cover a range relevant to particle transport in the heliosphere, a region amenable to direct exploration. Note that the particles are taken to be protons. All results are for speeds in units of c and lengths in units of λ. For example, in near-Earth space, the slab correlation length is estimated as 0.02 AU (Jokipii & Coleman 1968), and thus, $\lambda \approx 0.027$ AU near Earth; there are theories to estimate its dependence with heliospheric radius and latitude (e.g., Zank et al. 1998; Breech et al. 2008). In Table 1 we present results for parallel diffusion in terms of the mean free path, $\lambda_\parallel = 3\kappa_{zz}/v$. In place of the energy, we sometimes express results in terms of $R_{\rm L}/\lambda$, the Larmor radius $R_{\rm L} = \gamma mvc/(qB_0)$ divided by the parallel coherence scale of the turbulence. The ratio b/B_0 of the rms fluctuation to the mean field is set to 1 in runs 1–12, a reasonable value for the inner heliosphere, and is 10 in run 13, for the purpose of testing the SNL theory, which was designed for the case of $b \gg B_0$ (Stawicki 2005). The quantity f_s in the inner heliosphere has been estimated as 0.20 (Bieber et al. 1994) to 0.15 (Bieber et al. 1996), so we use the canonical value of 0.20 in most runs; other values are designed to explore properties of the theory. The nonaxisymmetry throughout the heliosphere is

TABLE 1

PARTICLE DIFFUSION COEFFICIENTS FROM SIMULATIONS AND NLGC THEORY

RUN	b_x/b_y	E (MeV)	f_s	T (λ/c)	SIMULATIONS κ_{xx}	SIMULATIONS κ_{yy}	SIMULATIONS κ_{xx}/κ_{yy}	SIMULATIONS $\lambda_\parallel$	NLGC THEORY κ_{xx}	NLGC THEORY κ_{yy}	NLGC THEORY κ_{xx}/κ_{yy}
1	1.00	100.0[b]	0.20	1×10^4	1.56×10^{-2}	1.66×10^{-2}	0.94	2.89	2.41×10^{-2}	2.41×10^{-2}	1.00
2	0.10	100.0	0.20	1×10^4	7.21×10^{-4}	5.88×10^{-2}	1.23×10^{-2}	4.33	8.61×10^{-4}	8.60×10^{-2}	1.00×10^{-2}
3	10.00	100.0	0.20	1×10^4	6.33×10^{-2}	7.00×10^{-4}	90.35	4.63	8.90×10^{-2}	8.90×10^{-4}	99.98
4	0.01	100.0	0.20	1×10^4	1.80×10^{-5}	1.11×10^{-1}	1.62×10^{-4}	6.04	1.78×10^{-5}	1.77×10^{-1}	1.01×10^{-4}
5	100.00	100.0	0.20	1×10^4	1.05×10^{-1}	1.71×10^{-5}	6161.22	5.67	1.69×10^{-1}	1.71×10^{-5}	9881.63
6	10.00	0.1[c]	0.20	1×10^6	5.13×10^{-4}	5.57×10^{-6}	92.10	1.45	1.52×10^{-3}	1.52×10^{-5}	99.92
7	10.00	1.0[d]	0.20	2×10^5	2.25×10^{-3}	2.27×10^{-5}	99.15	1.65	5.24×10^{-3}	5.24×10^{-5}	99.93
8	10.00	10.0[e]	0.20	2×10^4	1.28×10^{-2}	1.24×10^{-4}	102.63	2.64	2.22×10^{-2}	2.22×10^{-4}	99.96
9	10.00	1000.0[f]	0.20	1×10^4	1.82×10^{-1}	2.59×10^{-3}	70.20	9.96	2.54×10^{-1}	2.54×10^{-3}	99.98
10	10.00	100.0	0.01	1×10^5	7.59×10^{-2}	9.01×10^{-4}	84.20	64.24	...	...	...
11	10.00	100.0	0.80	2×10^4	9.28×10^{-3}	9.10×10^{-5}	102.00	1.20	2.76×10^{-2}	2.76×10^{-4}	99.99
12	10.00	100.0	0.99	2×10^5	8.58×10^{-4}[g]	8.10×10^{-6}[g]	105.86	0.78	2.14×10^{-2}	2.14×10^{-4}	99.99
13[a]	10.00	100.0	0.20	1×10^4	8.61×10^{-2}	8.07×10^{-4}	106.68	0.07	2.84×10^{-1}	2.85×10^{-3}	99.81

[a] For this run, $b = 10B_0$; in all other runs, $b = B_0$.
[b] Here, $E = 100$ MeV implies $v/c = 0.428$ and $R_L/\lambda = 0.099$.
[c] Here, $E = 0.1$ MeV implies $v/c = 0.015$ and $R_L/\lambda = 0.0031$.
[d] Here, $E = 1$ MeV implies $v/c = 0.046$ and $R_L/\lambda = 0.0097$.
[e] Here, $E = 10$ MeV implies $v/c = 0.145$ and $R_L/\lambda = 0.031$.
[f] Here, $E = 1000$ MeV implies $v/c = 0.875$ and $R_L/\lambda = 0.358$.
[g] Diffusion coefficient is decreasing, indicating subdiffusive behavior.

poorly known, but might conceivably be as great as 100 in the outer heliosphere, as explored in runs 4 and 5, due to different stretching of the solar wind plasma in the θ- and r-directions. For most runs, we use the more conservative value of $b_x/b_y = 10$.

We perform pairs of runs with inverted ratios (0.1 and 10; 0.01 and 100) in order to check the x-y interchange symmetry in the runs. The five pairs of particle diffusion coefficients related by this interchange symmetry (e.g., κ_{xx} and κ_{yy} for the axisymmetric run 1, κ_{xx} for run 2, and κ_{yy} for run 3) indicate that the results are reproducible to an uncertainty (standard deviation) of 4%. The comparison for runs 2–5 reveals that the NLGC theory results have an uncertainty of about 2.7% due to fluctuations in the input value $\lambda_\parallel$ from simulations, which in turn are reproducible to a standard deviation of 4.6%. Based on interchange symmetry, we estimate that the simulated field line diffusion coefficients, and hence the FLRW results, are reproducible to a standard deviation of 2.2%.

Figure 3*a* shows asymptotic perpendicular diffusion coefficients as a function of the nonaxisymmetry b_x/b_y. The simulation values are for runs 1–5, with other parameters fixed ($f_s = 0.2$ and $E = 100$ MeV, giving $R_L/\lambda = 0.099$). The NLGC theory provides a reasonable match to the simulation results over 4 orders of magnitude in b_x/b_y and in κ, with $\kappa_{NLGC}/\kappa_{sim}$ ranging from 0.99 for low κ to 1.61 for high κ. The FLRW model is too high, with $\kappa_{FLRW}/\kappa_{sim}$ ranging from 9 to 19.

The ratio κ_{xx}/κ_{yy} provides a sensitive test of the theories. The theory of field line diffusion (Ruffolo et al. 2006), and hence our expectations for the FLRW model of particle diffusion as well as

TABLE 2

SCALING OF PARTICLE DIFFUSION COEFFICIENTS FROM SIMULATIONS AND NLGC THEORY IN TERMS OF FIELD LINE DIFFUSION COEFFICIENTS

RUN	b_x/b_y	E (MeV)	f_s	D_x Simulation	D_x Theory[c]	D_y Simulation	D_y Theory[c]	$\kappa_{xx}/(vD_x)$ Simulation	$\kappa_{xx}/(vD_x)$ NLGC[e]	$\kappa_{yy}/(vD_y)$ Simulation	$\kappa_{yy}/(vD_y)$ NLGC[e]
1	1.00	100.0	0.20	4.05×10^{-1}	4.14×10^{-1}	3.94×10^{-1}	4.14×10^{-1}	0.090	0.139	0.098	0.143
2	0.10	100.0	0.20	1.53×10^{-2}	1.78×10^{-2}	1.56×10^{0}	1.78×10^{0}	0.110	0.131	0.088	0.129
3	10.00	100.0	0.20	1.53×10^{0}	1.78×10^{0}	1.57×10^{-2}	1.78×10^{-2}	0.096	0.136	0.104	0.132
4	0.01	100.0	0.20	3.73×10^{-4}	5.81×10^{-4}	4.88×10^{0}	5.81×10^{0}	0.113	0.112	0.053	0.084
5	100.00	100.0	0.20	4.74×10^{0}	5.81×10^{0}	3.55×10^{-4}	5.81×10^{-4}	0.052	0.083	0.112	0.113
6	10.00	0.1	0.20	1.53×10^{0}	1.78×10^{0}	1.57×10^{-2}	1.78×10^{-2}	0.023	0.068	0.024	0.066
7	10.00	1.0	0.20	1.53×10^{0}	1.78×10^{0}	1.57×10^{-2}	1.78×10^{-2}	0.032	0.074	0.031	0.072
8	10.00	10.0	0.20	1.53×10^{0}	1.78×10^{0}	1.57×10^{-2}	1.78×10^{-2}	0.057	0.100	0.055	0.097
9	10.00	1000.0	0.20	1.53×10^{0}	1.78×10^{0}	1.57×10^{-2}	1.78×10^{-2}	0.136	0.189	0.189	0.185
10	10.00	100.0	0.01	9.24×10^{-1}[b]	1.90×10^{0}	8.40×10^{-3}[b]	1.90×10^{-2}	0.192	...	0.251	...
11	10.00	100.0	0.80	1.32×10^{0}	1.20×10^{0}	1.22×10^{-2}	1.20×10^{-2}	0.016	0.049	0.017	0.053
12	10.00	100.0	0.99	7.58×10^{-1}	7.85×10^{-1}	7.61×10^{-3}	7.85×10^{-3}	0.003[d]	0.066	0.002[d]	0.066
13[a]	10.00	100.0	0.20	2.93×10^{1}	2.61×10^{1}	3.04×10^{-1}	2.61×10^{-1}	0.007	0.023	0.006	0.022

[a] For this run, $b = 10B_0$; in all other runs, $b = B_0$.
[b] Diffusion coefficient decreased and then became steady, indicating transient subdiffusive behavior followed by diffusion.
[c] Discrete theory of Ruffolo et al. (2006).
[d] Diffusion coefficient is decreasing, indicating subdiffusive behavior.
[e] NLGC discrete theory for κ, simulation for D.

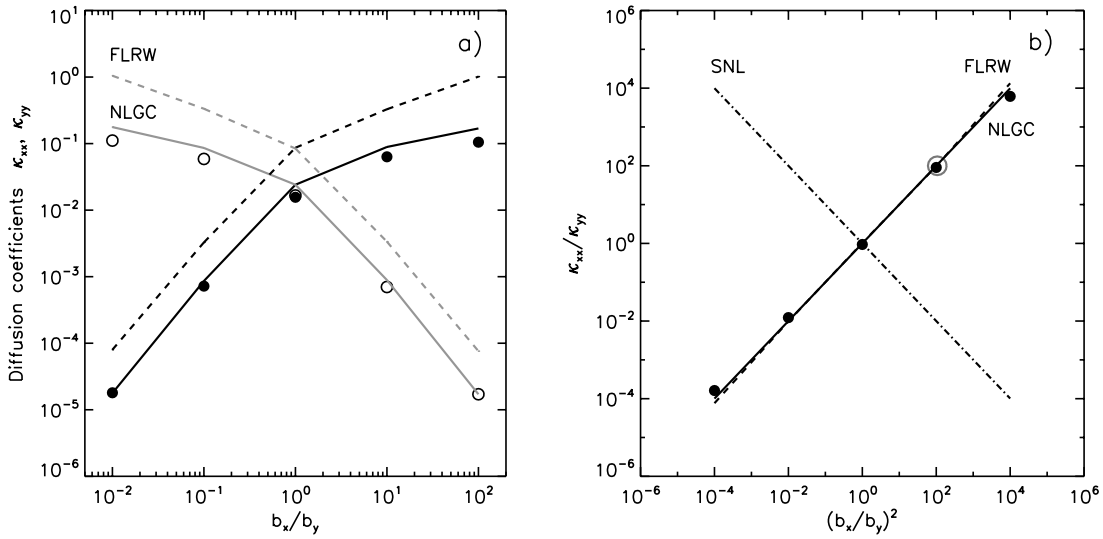

FIG. 3.—(*a*) Simulation results for particle diffusion coefficients κ_{xx} (*filled circles*) and κ_{yy} (*open circles*) as a function of nonaxisymmetry b_x/b_y for 100 MeV protons ($R_L/\lambda = 0.099$) in 20% slab + 80% 2D turbulence with $b = B_0$. Theoretical results are shown for NLGC (solid, black lines for κ_{xx} and solid, gray lines for κ_{yy}) and FLRW (dashed, black lines for κ_{xx} and dashed, gray lines for κ_{yy}, based on simulation results for field line diffusion coefficients). (*b*) Ratio κ_{xx}/κ_{yy} under the same conditions as above, including simulation results for $b = B_0$ (*filled circles*) and for $b = 10B_0$ (*open, gray circle*). The SNL prediction of Stawicki (2005), for $a_x = a_y$, is shown as a dash-dotted line.

NLGC theory, predict that $\kappa_{xx}/\kappa_{yy} = (b_x/b_y)^2$ (see § 2.2). The theory of Weinhorst et al. (2008), for a specific form of the power spectra, also yields this ratio (using a rotation angle of zero for alignment of the *x*- and *y*-axes with the nonaxisymmetric stretching, as in the present work). This expectation matches the simulation results reasonably well over 7 orders of magnitude in the ratio (Fig. 3*b*), to within ~20% for $10^{-2} \leq (b_x/b_y)^2 \leq 10^{+2}$ and ~50% for $(b_x/b_y)^2 = 10^{-4}$ or 10^{+4}.

The relation $\kappa_{xx}/\kappa_{yy} = (b_x/b_y)^2$ is exact in continuous theory for FLRW or NLGC. The values for discrete theory deviate slightly (at most 1.2% for NLGC) because the simulations employ a Fourier transform grid with equal spacings and box sizes in *x* and *y*. When using grid spacings and box sizes in *x* and *y* in the same ratio as b_x/b_y, this deviation was greatly reduced, but as a matter of choice we report results from simulations that are not "tailored" to the nonaxisymmetry in this way.

The simulations robustly show that $\kappa_{xx}/\kappa_{yy} \approx (b_x/b_y)^2$, varying little with the particle energy, the slab fraction f_s, and for $b/B_0 = 1$ or 10. At $b_x/b_y = 10$, the simulation value for κ_{xx}/κ_{yy} deviates from $(b_x/b_y)^2 = 100$ by at most 30% for all runs. In continuous theory the ratio should be independent of those quantities. The discrete theory values deviate by at most 0.2%.

Stawicki (2005) suggested that his SNL theory could be tested by simulations of particle diffusion. Assuming $a_x = a_y$ for both SNL and NLGC, we expect $(\kappa_{xx}/\kappa_{yy})_{SNL} = (\kappa_{xx}/\kappa_{yy})^{-1}_{NLGC}$ (see also § 2.1), as shown by the dot-dashed line in Figure 3*b*. The simulation results are in disagreement with the SNL prediction, either for $b = B_0$ (runs 1–5, the solid circles in Fig. 3*b*; similar results are obtained for runs 6–12) or $b = 10B_0$ (run 13, the open, gray circle in Fig. 3*b*); the latter run was performed in order to better test SNL in the limit of large b/B_0 for which it was designed.

Figure 4 shows results of perpendicular diffusion coefficients for runs 3 and 6–9 with varying energy (from 0.1 to 1000 MeV), with other parameter values fixed at $f_s = 0.2$ and $b/B_0 = 1$. Similar trends were found by Giacalone & Jokipii (1999) for axisymmetric fluctuations and by Pommois et al. (2007, see their Fig. 10) for axisymmetric and nonaxisymmetric fluctuations.

Both NLGC and FLRW theories capture the trend that κ values increase with energy, and the NLGC theory is again much closer to the simulation data. The agreement is much better for the higher energies in this range, with R_L not much smaller than λ. It is a known deficiency of NLGC theory that its agreement is worse at lower energy (Shalchi et al. 2004b; Minnie et al. 2007).

Both the simulations and the theoretical predictions indicate a rate of increase with R_L that slows down for the highest point; this is due to relativistic effects, as the highest point (for protons of $E = 1000$ MeV) has $v = 0.875c$. The trends are smoother when expressed in terms of v, because the strongest effect on κ is an approximate scaling with vD. The particle speed also has indirect effects on the physics, via the Larmor radius (as plotted in Fig. 4) and via the parallel scattering mean free path (see Fig. 5), to be discussed in more detail in § 3.4.

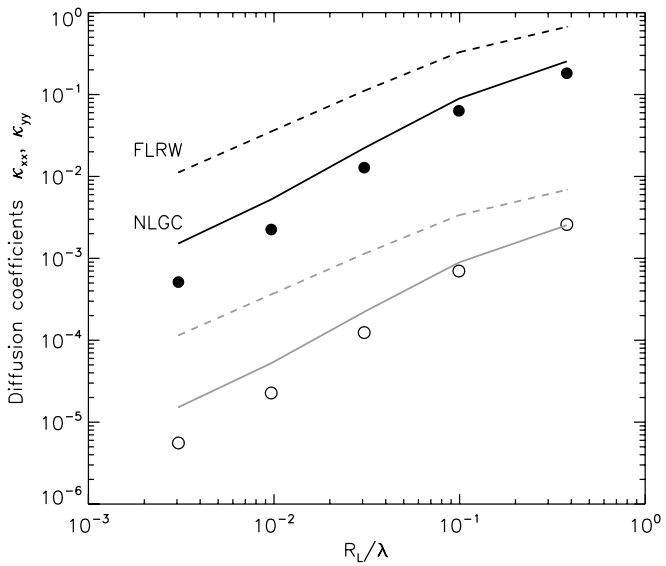

FIG. 4.—Simulation results for particle diffusion coefficients κ_{xx} (*filled circles*) and κ_{yy} (*open circles*) as a function of the Larmor radius divided by the turbulence scale length, R_L/λ (which is determined by the particle speed) in 20% slab + 80% 2D turbulence with $b_x/b_y = 10$ and $b = B_0$. Theoretical results are indicated as in Fig. 3*a*.

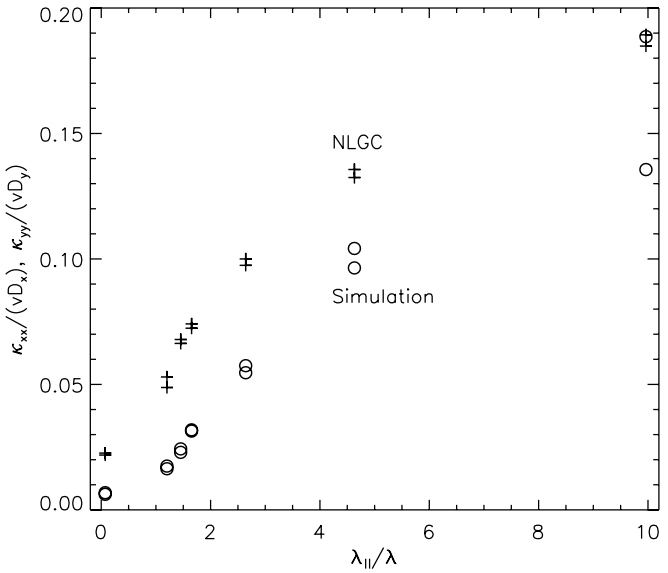

FIG. 5.—Simulation results and NLGC theory for the ratio $\kappa_{ii}/(vD_i)$, $i = x, y$, as a function of the parallel mean free path $\lambda_{\parallel}$ (in units of the parallel coherence scale λ), for all runs at $b_x/b_y = 10$ that exhibit field line and particle diffusion. Here $\lambda_{\parallel}$, which is also an input to the NLGC theory, and D_i are determined from simulations. Overall, the simulation data for κ_{ii} are well organized by vD_i over 4 orders of magnitude (see Fig. 3), and the ratio $\kappa_{ii}/(vD_i)$ is in turn well organized by $\lambda_{\parallel}$. The FLRW prediction is $\kappa_{ii}/(vD_i) = 0.5$; the NLGC theory comes closer to the simulation results and exhibits a similar trend with $\lambda_{\parallel}$.

3.3. *Reduced Dimensionality*

Next we vary the fluctuation anisotropy and study the approach to reduced dimensionality, in order to explore special behaviors and to compare with previous studies. Note that the theorem of Jokipii et al. (1993) and Jones et al. (1998) shows that for magnetic fields with an ignorable coordinate and certain other conditions, particles remain confined to flux surfaces. This could imply a qualitative difference between particle transport for, say, strictly 2D fields and nearly 2D fields that have some variation in the third dimension. To avoid this inherent effect of strictly reduced dimensionality, which is not expected to occur in nature, we perform simulations for magnetic fields with both slab and 2D fluctuations, setting the slab fraction to $f_s = 0.99$ to model the approach to 1D magnetic turbulence and $f_s = 0.01$ to model nearly 2D turbulence.

The results described in § 3.2 were for $f_s = 0.2$. For $f_s = 0.8$ (run 11) the results were qualitatively similar, forming a consistent trend in $\kappa/(vD)$ as a function of $\lambda_{\parallel}$ (see Fig. 5). In these cases, the perpendicular transport of particles comprises free streaming at short times, followed by transient subdiffusive behavior with $\langle \Delta x^2 \rangle \sim t^{\alpha}$ at α close to unity (Fig. 2) and then asymptotic diffusion. The field line random walk starts with free streaming and smoothly tends to diffusive behavior.

We note that a decrease in a running diffusion coefficient κ is not sufficient to indicate physically "subdiffusive" behavior. It is also necessary to check $\langle \Delta x^2 \rangle$ and $\langle \Delta y^2 \rangle$ computed from a fixed origin in time and their derivatives (slopes) as a function of t. In all our simulations of perpendicular transport, the slope rapidly increases to a high value, yielding an initial jump in $\langle \Delta x^2 \rangle$ and $\langle \Delta y^2 \rangle$, followed by a decrease in slope (subdiffusion). After that, the slope reaches a constant value for almost all cases (the exception is for $f_s = 0.99$ in run 10). However, a running diffusion coefficient such as $\kappa_{xx} \equiv \langle \Delta x^2 \rangle/(2t)$ will continue to decrease slightly with time because of the initial jump in $\langle \Delta x^2 \rangle$, sometimes conveying a misleading impression of subdiffusion.

Qin et al. (2002a) modeled nearly 1D fluctuations (varying mostly along z) using the 2D + slab model with 99.99% slab and 0.01% 2D energy. They found free streaming followed by asymptotic subdiffusion consistent with $\langle \Delta x^2 \rangle \propto \Delta t^{1/2}$, as predicted by models of compound subdiffusion (Getmantsev 1963; Urch 1977; Kóta & Jokipii 2000) from the viewpoint that particles are basically tied to field lines (see Fig. 1*b* and § 2.1). In the present work we can confirm compound subdiffusion for a slab fraction $f_s = 0.99$ (run 12), with the above form for $\langle \Delta x^2 \rangle$. No asymptotic diffusion regime is found, down to κ values 2 orders of magnitude below the prediction of the FLRW model and 1 order of magnitude below NLGC. The numerical values for κ_{xx} and κ_{yy} shown in Table 1 are averaged over the final one-fourth of the simulation duration $T = 2 \times 10^5 \lambda/c$.

Note that the field line random walk is still diffusive, which also holds in the case of pure slab fluctuations. Thus, the FLRW model predicts diffusive behavior for perpendicular particle diffusion, as does NLGC (which indeed assumes diffusion). Matthaeus et al. (2003) clearly pointed out this limitation of NLGC theory, and that asymptotic perpendicular transport is subdiffusive when there is insufficient "transverse complexity."

In the other limit of extreme anisotropy, strictly 2D turbulence (varying in the two perpendicular directions) should involve trapping of particles along ordered flux surfaces that are independent of z. For the 2D component of turbulence, a flux surface is at a constant value of $a(x, y)$. At 1% slab energy (run 10), the field line random walk exhibits free streaming followed by a transient subdiffusion phase. At $\Delta z \sim 100\lambda$, the derivative of $\langle \Delta x^2 \rangle$ with respect to Δz becomes constant to within the resolution of the simulations. As shown in Table 2, the asymptotic field line diffusion coefficient is roughly one-half that predicted by the theory of Ruffolo et al. (2006). The transient subdiffusive regime was not anticipated in that theory.

Furthermore, the NLGC theory for particle transport breaks down in the sense of not having a solution with positive κ_{xx} and κ_{yy}. Nevertheless, the perpendicular transport does exhibit asymptotic diffusion, with κ values forming a consistent trend as a function of f_s. The FLRW model can be applied and is in error by a factor of 5, which is typical for the runs with 100 MeV particles.

The NLGC theory of particle diffusion (and extensions thereof) and the theory of field line diffusion for nonaxisymmetric fluctuations (Ruffolo et al. 2006) make use of Corrsin's independence hypothesis (Corrsin 1959) that the ensemble average Lagrangian correlation between fluctuations at two points along a trajectory is determined by independent statistics of the trajectory and of the ensemble average Eulerian correlation for the displacement between the two points (see also Taylor & McNamara 1971; Matthaeus et al. 1995). The transient subdiffusive regime of the field line random walk indicates that Corrsin's hypothesis is partially violated in the case of nearly closed trajectories in the x-y plane. As an instructive example, consider the subensemble of field lines starting on flux surfaces that are traversed over a period L in the z-direction, and suppose that the Eulerian correlation is always nonnegative. Then the Lagrangian correlation from Corrsin's hypothesis will also be nonnegative, indicating a diffusive random walk with no memory of its starting location, whereas the actual Lagrangian correlation is both positive and negative with period L, after which the field lines return to their starting (x, y) locations. In practice the full ensemble comprises many values of L, the periodic motion is not exact, and field lines can diffuse away from their original equipotential contour (at a reduced rate; see Chuychai et al. 2007), so the overall violation of Corrsin's hypothesis is not so dramatic. Nevertheless, the partial failure of Corrsin's hypothesis can explain why those theories of field line

and particle diffusion do not properly apply to the case of nearly 2D fluctuations.

3.4. *Scaling of κ with vD*

In Table 2 we see that to first order, our values of κ_{ii} from simulations and NLGC theory scale as vD_i, for $i = x, y$. The ratio κ_{xx}/κ_{yy} is close to $(b_x/b_y)^2$, as is the ratio D_x/D_y. Indeed, it is natural to view that κ is different in the x- and y-directions because of the difference in D for the field lines. The scaling of κ with vD is assumed in the FLRW model and also holds for NLGC in the limit of long $\lambda_\parallel$, although with different prefactors for fluctuations dominated by the slab or 2D component (see § 2.3).

All of our results for asymptotic perpendicular diffusion of particles have a ratio $\kappa_{ii}/(vD_i)$ to within an order of magnitude of 0.05, for κ_{ii} ranging over 4 orders of magnitude. The ratio would be 0.5 in the FLRW model. The ratio varies systematically with particle energy, as seen in Figure 4 [comparing points for simulations with the dashed line for FLRW with $\kappa_{ii} = (1/2)vD_i$].

Minnie et al. (2008) note that the limit of high energy corresponds to weak scattering and show results for the dependence of $\lambda_\perp = 3\kappa_\perp/v$ on $\lambda_\parallel$ for axisymmetric fluctuations (with fixed D). Thus, we pursue the idea that the particle energy affects $\kappa_{ii}/(vD_i)$ for nonaxisymmetric turbulence through its effect on $\lambda_\parallel$, which is indeed an input for the NLGC theory. Figure 5 shows $\kappa_{ii}/(vD_i)$ from simulation results (*circles*) and NLGC theory (*plus signs*) for both $i = x, y$, compared with $\lambda_\parallel = 3\kappa_{zz}/v$ from simulations (note the linear scale). In most cases the ratio is very similar for the x- and y-directions, except for the rightmost values where the simulation's ratio is substantially higher in the y-direction. Figure 5 includes results for all runs at $b_x/b_y = 10$ that exhibit asymptotic perpendicular diffusion. From low to high $\lambda_\parallel$, these include run 13 ($b/B_0 = 10$, $f_s = 0.2$), run 12 ($b/B_0 = 1$, $f_s = 0.99$), and run 11 ($b/B_0 = 1$, $f_s = 0.8$), all at $E = 100$ MeV, and runs 6, 7, 8, 3, and 9 for increasing energy at $b/B_0 = 1$, $f_s = 0.2$. For this wide variety of parameter values, the simulation results are well organized by $\lambda_\parallel$.

The NLGC results are also organized by $\lambda_\parallel$ and show an increasing trend, with a hint of saturation at high $\lambda_\parallel$ as explained by Minnie et al. (2008) and § 2.3 of the present work. One may view that as $\lambda_\parallel$ decreases from a high value, it causes decorrelation of the perpendicular particle motion at earlier times and, thus, plays more of a role. That role is evidently not perfectly modeled by NLGC, although the fit to the simulation results is much better than that of FLRW, for which the ratio is 0.5.

We note as an aside that when the nonaxisymmetry b_x/b_y is more different from unity, $\lambda_\parallel$ is found to increase in the simulation results. To explain that effect on parallel transport is beyond the scope of the present work. At the same time, $\kappa_{ii}/(vD_i)$ is roughly constant or decreasing. Thus, the organization of $\kappa_{ii}/(vD_i)$ with $\lambda_\parallel$ is best understood as applying for fixed b_x/b_y.

4. TIME HISTORY OF PERPENDICULAR TRANSPORT

In this section we present a heuristic model to describe the time history of perpendicular transport, from free streaming to subdiffusion and asymptotic diffusion (Fig. 2). This time sequence applies to all runs in the present study except run 12, the nearly 1D case with 99% slab turbulent energy (see § 3.3), which exhibits asymptotic subdiffusion in the form of compound subdiffusion. For asymptotic diffusion or subdiffusion at long times, one can use the Taylor-Green-Kubo formalism (see § 2.1 and Kóta & Jokipii 2000). To examine earlier times, we use a more general formalism, following Ruffolo et al. (2004). We also include the physics of backtracking (see Fig. 1) in a heuristic way to account for the subdiffusion.

The perpendicular displacement of a particle in the x-direction as a function of time t is given by

$$\Delta x \equiv x(t) - x(0) = \int_0^t v_x(t')dt'. \tag{46}$$

Then the mean squared displacement is given by the double integral

$$\left\langle \Delta x^2 \right\rangle = \int_0^t \int_0^t \langle v_x(t')v_x(t'')\rangle dt'\, dt''. \tag{47}$$

This can be rewritten in terms of $\Delta t \equiv t'' - t'$, and with the assumption of statistically homogeneous fluctuations,

$$\left\langle \Delta x^2 \right\rangle = \int_0^t \int_{-t'}^{t-t'} \langle v_x(0)v_x(\Delta t)\rangle d\Delta t\, dt'. \tag{48}$$

At this point, to study the asymptotic (long-time) behavior, one could obtain the Taylor-Green-Kubo (TGK) formalism (e.g., Kubo 1957) by setting the limits of Δt integration to infinity, which makes the t' integration trivial,

$$\kappa_{xx} \equiv \frac{\left\langle \Delta x^2 \right\rangle}{2t} = \frac{1}{2}\int_{-\infty}^{\infty} \langle v_x(0)v_x(\Delta t)\rangle d\Delta t. \tag{49}$$

The TGK approximation is valid when the correlation function $\langle v_x(0)v_x(\Delta t)\rangle$ approaches zero for large time displacements Δt and when t is much larger than the decorrelation time. It is not valid for a long decorrelation time, or when the particle has "memory" of its transport history over the timescale of interest, t. In our case of subdiffusion (as in Fig. 2), the "memory" is that the particle can sometimes backtrack over a similar path because it is still following a similar field line.

Therefore, we continue from equation (48). We propose a heuristic formula for the velocity correlation,

$$\langle v_x(0)v_x(\Delta t)\rangle = \alpha \exp\left(-\frac{|\Delta t|}{t_1}\right) - \beta \exp\left(-\frac{|\Delta t|}{t_s}\right) \tag{50}$$

for positive α and β. The first term on the right-hand side is a standard positive correlation term with a decorrelation time that we call t_1 because it determines the onset time of first diffusion (Fig. 1*a*). Physically, if this were the only term, the particle velocity would decorrelate (e.g., due to the random walk of the guiding field line) and thereafter have no memory of its initial velocity. This term alone can describe a simple diffusive random walk.

The second term on the right-hand side of equation (50) is negative with a much smaller magnitude ($\beta \ll \alpha$) but a much longer timescale, t_s. This term leads to transient subdiffusive behavior, and t_s determines the duration of the subdiffusion before it settles into asymptotic diffusion. Physically, the negative correlation represents backtracking along a similar path. This causes a net negative correlation with the initial velocity, as there are some trajectories that extend further along the field line, undergo parallel scattering to reverse v_z, and then arrive back to the initial location after a time Δt. Such trajectories return with the reverse sign of v_x (see Fig. 1*b*). The case of two reversals of v_z to return to the initial location with a positive correlation is considered less likely, so the net result of backtracking is a negative correlation. It is not clear what timescale t_s, or indeed what key mechanism, is needed for the particle to leave its guiding field line, to follow a

field line sufficiently distinct (due to "transverse complexity"; Matthaeus et al. 2003) for the backtracking effect to be reduced. Pending improved theoretical understanding, we retain t_s as an undetermined parameter.

Directly integrating equation (48), we obtain

$$\langle \Delta x^2 \rangle = 2\alpha t_1 \left\{ t - t_1 \left[1 - \exp\left(-\frac{t}{t_1} \right) \right] \right\} - 2\beta t_s \left\{ t - t_s \left[1 - \exp\left(-\frac{t}{t_s} \right) \right] \right\}, \quad (51)$$

which implies that

$$\kappa_{xx} = \alpha t_1 \left\{ 1 - \frac{t_1}{t} \left[1 - \exp\left(-\frac{t}{t_1} \right) \right] \right\} - \beta t_s \left\{ 1 - \frac{t_s}{t} \left[1 - \exp\left(-\frac{t}{t_s} \right) \right] \right\}. \quad (52)$$

Here κ_{xx} rises quickly (over time t_1) and then falls gradually (over time t_s) to its asymptotic level $\kappa_a = \alpha t_1 - \beta t_s$. Replacing α and β with the more pertinent quantities $\kappa_1 = \alpha t_1$ (the diffusion coefficient obtained from the first term only) and κ_a, we obtain

$$\kappa = \kappa_1 \left\{ 1 - \frac{t_1}{t} \left[1 - \exp\left(-\frac{t}{t_1} \right) \right] \right\} - (\kappa_1 - \kappa_a) \left\{ 1 - \frac{t_s}{t} \left[1 - \exp\left(-\frac{t}{t_s} \right) \right] \right\}. \quad (53)$$

We experimented with fitting simulation data for κ_{xx} and κ_{yy} as independent functions of t. Figure 2 shows such fits (*blue lines*) for run 3, chosen because it uses the "baseline" values for all parameters. Here the value of κ_a was fixed to the average value of κ over the last quarter of the run, as reported in Table 1, κ_1 and t_1 were fixed to match κ and t at the peak, and t_s was allowed to vary. Such fits were reasonably successful in matching time profiles for this and other runs. However, the statistics are insufficient to allow a precise determination of the timescale t_s.

In conclusion, our heuristic model based on equation (50) yields a fit function, equation (53), that provides a reasonable match to the time profile of free streaming, subdiffusion, and asymptotic diffusion in the perpendicular transport of particles. We believe that equation (50) captures the key physics of long-term negative velocity correlations due to backtracking and provides a simple explanation of the subdiffusion (which is not compound subdiffusion with $\langle \Delta x^2 \rangle \propto t^{1/2}$) and its transition to asymptotic diffusion. Hopefully further work will develop a theory based on first principles that can provide a prescription for the transition timescale t_s.

This heuristic model does not replace NLGC theory. NLGC aims to find the value of κ for asymptotic diffusion, with more fundamental assumptions, and can do so with some accuracy. This heuristic model does provide some insight that the asymptotic value of κ is reduced from that of first diffusion, κ_1, due to the effect of backtracking, which at late times is subsumed into the melange of random walk trajectories. As a reality check, if κ_1 is to be interpreted as a coefficient of first diffusion, it should roughly correspond to the FLRW value, $\kappa_{\rm FLRW}$. Then the peak value of κ (which includes a negative contribution from the backtracking term) should be below $\kappa_{\rm FLRW}$, which is usually the case. This also helps explain why the $\kappa_{\rm NLGC}$ for asymptotic diffusion is always lower than $\kappa_{\rm FLRW}$. Mathematically, the backtracking term in equation (50) reduces the TGK integral in equation (49) for the asymptotic diffusion coefficient. It should also be noted that this heuristic model does not apply to subdiffusion for nearly 1D turbulence, such as our run 12, where the simulations do yield subdiffusion in the form of compound subdiffusion, with no transition to asymptotic diffusion.

5. DISCUSSION

The simulation data for the asymptotic perpendicular diffusion of energetic charged particles in 3D turbulence are fit reasonably well by the NLGC theory. For the parameters used in this study, which may apply to energetic particles in the heliosphere, diffusion coefficients from the FLRW model [$\kappa_{\rm FLRW} = (1/2)vD$, for field line diffusion coefficients D determined by either simulations or theory] are typically 1–2 orders of magnitude too high. (Note that Minnie et al. [2007] found a smaller discrepancy for simulations with a smaller relative fluctuation amplitude b/B_0.) Dividing $\kappa_{\rm FLRW}$ by 10, i.e., using $\kappa = 0.05vD$, works to within an order of magnitude for all our runs with asymptotic diffusion (see Table 2). This scaling of κ with vD applies over 4 orders of magnitude in κ. NLGC theory provides a further improvement over that scaling, showing a systematic trend of $\kappa/(vD)$ with $\lambda_\parallel$ that is similar to that of the simulation data (see § 3.4 and Fig. 5). Nevertheless, the values of $\kappa_{\rm NLGC}$ are almost always somewhat too high in comparison with simulation results.

This is a justification of the conceptual framework of NLGC theory, in which the guiding center locally follows the field line random walk but is liberated from compound subdiffusion by cross field motions. The limiting behavior of NLGC for a long parallel mean free path $\lambda_\parallel$ (i.e., weak parallel scattering) can help explain the approximate scaling of κ with vD. In that limit, both κ and D are determined by the same mechanisms for decorrelation of the random walk (of particles and field lines, respectively), so that $\kappa \sim v_{z,\rm rms} D$ (§ 2.3). As $\lambda_\parallel$ decreases, it causes earlier decorrelation and reduces the value of κ.

The present work has explored the perpendicular transport of particles in three "directions": nonaxisymmetry, anisotropy, and time. Regarding the effects of nonaxisymmetry, our clearest result is that $\kappa_{xx}/\kappa_{yy} \approx (b_x/b_y)^2$. [In fact, we confirm that $D_x/D_y \approx (b_x/b_y)^2$ (see also Ruffolo et al. 2006).] The NLGC and FLRW models also yield this relation for κ_{xx}/κ_{yy} (see Fig. 3), as does the theoretical model of Weinhorst et al. (2008). However, the SNL theory of Stawicki (2005) is in conflict with these simulation data, at least when using $a_x = a_y$ (as we do for NLGC), because that theory instead predicts the inverse, $\kappa_{xx}/\kappa_{yy} \approx (b_x/b_y)^{-2}$.

We note that the nonaxisymmetric FLRW was examined by Pommois et al. (1999), who reported $D_x/D_y \sim \ell_x/\ell_y$, for their scale lengths ℓ_i, and by Pommois et al. (2001), who reported approximately $D_x/D_y \sim (\ell_x/\ell_y)^{0.8}$. However, a comparison with our results is tricky. We use a two-component 2D + slab model of turbulence, in which two components of reduced dimensionality are summed, giving a field that varies in three dimensions at a low computational cost (§ 2.2). This allows us to provide comprehensive coverage of $\boldsymbol{k}$-space, with many Fourier modes. The work by Pommois et al. (1999, 2001), and their subsequent work, uses "ellipsoidal" turbulence (with equal power over ellipsoids in $\boldsymbol{k}$-space) that is unpolarized, evaluated by "band spectra." Because the turbulence is not polarized, a large ratio of ℓ_x/ℓ_y (at $\ell_z = \ell_y$) implies at most a field ratio of $b_x/b_y = 2$ (see Table 1 of Pommois et al. 1999). Then their dynamic range of a factor of 10 in ℓ_x/ℓ_y corresponds to a factor of 2 in b_x/b_y. According to Matthaeus et al. (2007), for 2D turbulence $D_x/D_y = (b_x/b_y)(\tilde{\lambda}_x/\tilde{\lambda}_y)$, and the ratio of ultrascales, $\tilde{\lambda}_x/\tilde{\lambda}_y = \xi$, is in turn equal to b_x/b_y. To generalize

this to 3D unpolarized turbulence and evaluate the ultrascales is beyond the scope of this work, so it is difficult to interpret the dependence of D_x/D_y on ℓ_x/ℓ_y from Pommois et al. (1999, 2001), as well as the dependence of κ values as a function of nonaxisymmetry as reported by Pommois et al. (2007).

Our findings for turbulence that approaches reduced dimensionality are somewhat at variance with previous reports in the literature. For nearly 1D turbulence (99% slab energy; run 12), we obtain asymptotic subdiffusion in the perpendicular directions as reported in earlier studies (Qin et al. 2002a; Zimbardo et al. 2006), and the NLGC and FLRW models are inapplicable. However, in the parallel direction, for κ_{zz}, we find a prolonged but steady approach from free streaming to asymptotic diffusion. Previous work (Pommois et al. 2005, 2007; Zimbardo et al. 2006) has reported that the parallel transport is superdiffusive. Based on their graphs, it appears that if their simulations are continued for longer durations, they may agree with our result of a smooth transition from free streaming to asymptotic diffusion.

For nearly 2D turbulence (1% slab energy; run 10), it is interesting that the field line random walk undergoes free streaming, then subdiffusion, followed by asymptotic diffusion. This temporary epoch of subdiffusion is evidently related to the near confinement to ordered flux surfaces. The escape from such confinement to reach a diffusive process may be related to percolation processes reported previously for very high Kubo numbers (Isichenko 1991; Reuss & Misguich 1996; Zimbardo et al. 2000).

At the same time that our previous theory (Ruffolo et al. 2006) and prediction of Bohm diffusion ($D \propto b/B_0$) break down for nearly 2D turbulence, NLGC theory also fails to yield positive values of κ_{xx} and κ_{yy}. Nevertheless, simulations of the perpendicular transport of particles indicate asymptotic diffusion, albeit after a long time duration. Thus, one can say that NLGC theory works well only for essentially 3D turbulence, for which it was designed.

In our final direction, to consider earlier times, we provide a heuristic model with two terms in the velocity correlation function: a positive correlation due to initial coherence and a long-term negative correlation due to backtracking (see Fig. 1*b*). This yields a functional form for the diffusion coefficient that can match the simulation data for the initial epoch of free streaming and subdiffusion (that is not in the form of compound subdiffusion) followed by asymptotic diffusion. A challenge for future work is to understand the mechanism and timescale for particles to "cross" field lines, or more specifically, to follow field lines with a different global trajectory than the original field lines.

This research was partially supported by the Thailand Research Fund, NASA grants NNX 07-AH73G (Heliospheric Guest Investigator) and NNX 08-AI47G (Heliophysics Theory), and NSF grants ATM 05-39995 and ATM 07-52135 (Solar, Heliospheric, and Interplanetary Environment).

REFERENCES

Belcher, J. W., & Davis, L., Jr. 1971, J. Geophys. Res., 76, 3534
Bieber, J. W., & Matthaeus, W. H. 1997, ApJ, 485, 655
Bieber, J. W., Matthaeus, W. H., Shalchi, A., & Qin, G. 2004, Geophys. Res. Lett., 31, L10805
Bieber, J. W., Matthaeus, W. H., Smith, C. W., Wanner, W., Kallenrode, M.-B., & Wibberenz, G. 1994, ApJ, 420, 294
Bieber, J. W., Wanner, W., & Matthaeus, W. H. 1996, J. Geophys. Res., 101, 2511
Breech, B., Matthaeus, W. H., Minnie, J., Bieber, J. W., Oughton, S., Smith, C. W., & Isenberg, P. A. 2008, J. Geophys. Res., in press
Burger, R. A., & Hattingh, M. 1998, ApJ, 505, 244
Chandran, B. D. G., & Cowley, S. C. 1998, Phys. Rev. Lett., 80, 3077
Chuychai, P., Ruffolo, D., Matthaeus, W. H., & Meechai, J. 2007, ApJ, 659, 1761
Corrsin, S. 1959, in Atmospheric Diffusion and Air Pollution, ed. F. Frenkel & P. Sheppard (New York: Academic), 161
Dasso, S., Milano, L. J., Matthaeus, W. H., & Smith, C. W. 2005, ApJ, 635, L181
Getmantsev, G. G. 1963, Soviet Astron., 6, 477
Giacalone, J., & Jokipii, J. R. 1999, ApJ, 520, 204
Giacalone, J., Jokipii, J. R., & Mazur, J. E. 2000, ApJ, 532, L75
Gray, P. C., Pontius, D. H., Jr., & Matthaeus, W. H. 1996, Geophys. Res. Lett., 23, 965
Isichenko, M. B. 1991, Plasma Phys. Controlled Fusion, 33, 809
Jokipii, J. R. 1966, ApJ, 146, 480
———. 1973, ApJ, 182, 585
Jokipii, J. R., & Coleman, P. J. 1968, J. Geophys. Res., 73, 5495
Jokipii, J. R., Kóta, J., & Giacalone, J. 1993, Geophys. Res. Lett., 20, 1759
Jokipii, J. R., Kóta, J., Giacalone, J., Horbury, T. S., & Smith, E. J. 1995, Geophys. Res. Lett., 22, 3385
Jokipii, J. R., & Parker, E. N. 1968, Phys. Rev. Lett., 21, 44
Jones, F. C., Jokipii, J. R., & Baring, M. G. 1998, ApJ, 509, 238
Kóta, J., & Jokipii, J. R. 2000, ApJ, 531, 1067
Kubo, R. 1957, J. Phys. Soc. Japan, 12, 570
le Roux, J. A., & Webb, G. M. 2007, ApJ, 667, 930
Matthaeus, W. H., Bieber, J. W., Ruffolo, D., Chuychai, P., & Minnie, J. 2007, ApJ, 667, 956
Matthaeus, W. H., Goldstein, M. L., & Roberts, D. A. 1990, J. Geophys. Res., 95, 20673
Matthaeus, W. H., Gray, P. C., Pontius, D. H., Jr., & Bieber, J. W. 1995, Phys. Rev. Lett., 75, 2136
Matthaeus, W. H., Qin, G., Bieber, J. W., & Zank, G. 2003, ApJ, 590, L53
Minnie, J., Bieber, J. W., Matthaeus, W. H., & Burger, R. A. 2007, ApJ, 663, 1049
Minnie, J., Burger, R. A., Parhi, S., Matthaeus, W. H., & Bieber, J. W. 2005, Adv. Space Res., 35, 543
Minnie, J., Matthaeus, W. H., Bieber, J. W., Ruffolo, D., & Burger, R. A. 2008, ApJ, submitted
Parker, E. N. 1958, ApJ, 128, 664
Pommois, P., Veltri, P., & Zimbardo, G. 1999, Phys. Rev. E, 59, 2244
———. 2001, Phys. Rev. E, 63, 066405
Pommois, P., Zimbardo, G., & Veltri, P. 2005, Adv. Space Res., 35, 647
———. 2007, Phys. Plasmas, 14, 012311
Press, W. H., Teukolsky, S. A., Vetterling, W. T., & Flannery, B. P. 1992, Numerical Recipes in FORTRAN: The Art of Scientific Computing (Cambridge: Cambridge Univ. Press)
Qin, G. 2007, ApJ, 656, 217
Qin, G., Matthaeus, W. H., & Bieber, J. W. 2002a, Geophys. Res. Lett., 29, 7
———. 2002b, ApJ, 578, L117
Rechester, A. B., & Rosenbluth, M. M. 1978, Phys. Rev. Lett., 40, 38
Reuss, J.-D., & Misguich, J. H. 1996, Phys. Rev. E, 54, 1857
Ruffolo, D., Chuychai, P., & Matthaeus, W. H. 2006, ApJ, 644, 971
Ruffolo, D., Matthaeus, W. H., & Chuychai, P. 2003, ApJ, 597, L169
———. 2004, ApJ, 614, 420
Saur, J., & Bieber, J. W. 1999, J. Geophys. Res., 104, 9975
Shalchi, A. 2006, A&A, 453, L43
Shalchi, A., Bieber, J. W., & Matthaeus, W. H. 2004a, ApJ, 615, 805
Shalchi, A., Bieber, J. W., Matthaeus, W. H., & Qin, G. 2004b, ApJ, 616, 617
Shalchi, A., Bieber, J. W., Matthaeus, W. H., & Schlickeiser, R. 2006, ApJ, 642, 230
Shalchi, A., & Kourakis, I. 2007, A&A, 470, 405
Skilling, J., McIvor, I., & Holmes, J. A. 1974, MNRAS, 167, 87P
Stawicki, O. 2005, Adv. Space Res., 35, 547
Stone, E. C., Cummings, A. C., McDonald, F. B., Heikkila, B. C., Lal, N., & Webber, W. R. 2005, Science, 309, 2017
Taylor, J. B., & McNamara, B. 1971, Phys. Fluids, 14, 1492
Tooprakai, P., Chuychai, P., Minnie, J., Ruffolo, D., Bieber, J. W., & Matthaeus, W. H. 2007, Geophys. Res. Lett., 34, L17105
Urch, I. H. 1977, Ap&SS, 46, 389
Weinhorst, B., Shalchi, A., & Fichtner, H. 2008, ApJ, 677, 671
Zank, G. P., Matthaeus, W. H., Bieber, J. W., & Moraal, H. 1998, J. Geophys. Res., 103, 2085
Zimbardo, G., Pommois, P., & Veltri, P. 2004, J. Geophys. Res., 109, A02113
———. 2006, ApJ, 639, L91
Zimbardo, G., Veltri, P., & Pommois, P. 2000, Phys. Rev. E, 61, 1940